

Stabilization-free Virtual Element Method for 2D second order elliptic equations

*Original*

Stabilization-free Virtual Element Method for 2D second order elliptic equations / Berrone, S., Borio, A., Fassino, D., Marcon, F.. - In: COMPUTER METHODS IN APPLIED MECHANICS AND ENGINEERING. - ISSN 0045-7825. - 438-A:(2025), pp. 1-24. [10.1016/j.cma.2025.117839]

*Availability:*

This version is available at: 11583/2997574 since: 2025-02-18T10:50:10Z

*Publisher:*

Elsevier

*Published*

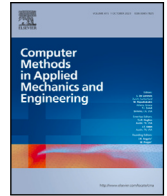
DOI:10.1016/j.cma.2025.117839

*Terms of use:*

This article is made available under terms and conditions as specified in the corresponding bibliographic description in the repository

*Publisher copyright*

(Article begins on next page)



# Stabilization-free Virtual Element Method for 2D second order elliptic equations

Stefano Berrone , Andrea Borio , Davide Fassino , Francesca Marcon \*

Dipartimento di Scienze Matematiche, Politecnico di Torino, Corso Duca degli Abruzzi 24, Torino, 10129, TO, Italy

## ARTICLE INFO

### MSC:

65N12

65N15

65N30

### Keywords:

Virtual Element Methods

RCD problems

Polygonal meshes

Structure-preserving formulation

## ABSTRACT

In this work, we present and analyze a Stabilization-free Virtual Element high order scheme for 2D second order elliptic equation. This method is characterized by the definition of new polynomial projections that allow the definition of structure-preserving schemes. We provide a necessary and sufficient condition on the polynomial projection space that ensure the well-posedness of the scheme and we derive optimal a priori error estimates. Several numerical tests assess the stability of the method and the robustness in solving problems characterized by anisotropies.

## 1. Introduction

Virtual Element Methods (VEMs) [1,2] are numerical methods for the solution of partial differential equations that allow the use of general polygonal and polyhedral meshes, which is a topic of large interest in several engineering applications. The main idea of this family of methods is to define discrete functional spaces containing polynomials and other unknown functions, in order to satisfy the required Sobolev regularity of the scheme and use classic sets of degrees of freedom. The problem's differential operator is then approximated by the sum of a bilinear form providing consistency on polynomials and another bilinear form ensuring stability whose choice remains somehow arbitrary during the years. A large literature on the role of the stability term has been produced in the last years, in particular it has been shown that its isotropic nature can causes some issues in applications characterized by advection-dominated regime [3,4]. Furthermore, in the classical a posteriori error analysis [5,6] the stability term appears on the right-hand side and it does not need to reduce under mesh refinement, bringing some issues in the adaptive theory. The interest in the topic of stabilization is proven by a large number of recent works that have been published, we mention for instance [7] where a reduced basis method to design the stabilization term is proposed, [8–10] where bounds for the stability terms used in the a posteriori error analysis are presented, [11] where a quantitative study of the parameters involved in the stabilization is performed, and [12] where authors show the sensitivity of the solution of eigenvalue problems to variable parameters included in the discretization matrices.

More recently, new  $H^1$ -conforming and  $H(\text{div})$ -conforming VEM schemes were proposed in [13–17], based on consistent and stable polynomial projections of basis functions, thus allowing the definition of coercive discrete bilinear forms based only on polynomial projections, that preserve the structure of the problem's operator. These methods have then been applied in a lot of contests: problems characterized by anisotropies [18], elasticity problems [19–21], convection-dominated problems [22], finite strain problems [23], and for bi-dimensional elastoplastics models [24,25].

\* Corresponding author.

E-mail addresses: [stefano.berrone@polito.it](mailto:stefano.berrone@polito.it) (S. Berrone), [andrea.borio@polito.it](mailto:andrea.borio@polito.it) (A. Borio), [davide.fassino@polito.it](mailto:davide.fassino@polito.it) (D. Fassino), [francesca.marcon@polito.it](mailto:francesca.marcon@polito.it) (F. Marcon).

<https://doi.org/10.1016/j.cma.2025.117839>

Received 16 September 2024; Received in revised form 18 December 2024; Accepted 7 February 2025

Available online 16 February 2025

0045-7825/© 2025 The Authors. Published by Elsevier B.V. This is an open access article under the CC BY-NC-ND license (<http://creativecommons.org/licenses/by-nc-nd/4.0/>).

In this paper, we deal with a 2D  $H^1$ -conforming Virtual Element Method discretization and generalize the scheme presented in [17] to allow for arbitrary polynomial accuracy of the method. Also, the scheme is formulated for a general second order elliptic PDE with variable coefficients. The proposed method of degree  $k$  is based on high-degree polynomial projections, whose divergence is of degree  $k-2$ . We identify a necessary and sufficient condition on the polynomial space such that the projection operator is stable and thus the method is well-posed and optimal a priori error estimates can be derived. We notice that the polynomial degree of such projections depends on the element's geometry. Hence, an algorithm is proposed to compute the optimal polynomial projection. Numerical tests are presented to confirm the robustness of the presented method. In particular, we select several polygonal shapes to assess the stability of the method for different accuracy orders  $k$ . Furthermore, we propose comparisons with a standard VEM approach to problems characterized by anisotropies.

The paper is structured as follows. The model problem is presented in Section 2. Section 3 is devoted to the presentation of the discrete scheme and the definition of the new higher-order polynomial projections. Well-posedness of the discrete problem is discussed in Section 4. Section 5 shows the  $L^2$  and  $H^1$  a priori error estimates. The computation of the projection is shown in Section 6. Finally, Section 7 contains the numerical tests.

## 2. Model problem

Let  $\Omega \subset \mathbb{R}^2$  be a bounded open set. We are interested in solving the following general second-order problem:

$$\begin{cases} \nabla \cdot (-\mathcal{K} \nabla u + \beta u) + \gamma u = f & \text{in } \Omega, \\ u = 0 & \text{on } \partial\Omega, \end{cases} \quad (1)$$

where  $\beta \in (L^\infty(\Omega))^2$  with  $\nabla \cdot \beta = 0$ , and  $\gamma \in L^\infty(\Omega)$  and non negative on  $\Omega$ , the loading term  $f \in L^2(\Omega)$ . We assume the symmetric diffusive tensor  $\mathcal{K} \in (L^\infty(\Omega))^{2 \times 2}$  and satisfy:

$$\mathcal{K}_0 |v|^2 \leq v \cdot \mathcal{K}(x)v \leq \mathcal{K}_1 |v|^2, \quad \forall v \in \mathbb{R}^2, \quad \forall x \in \Omega, \quad (2)$$

where  $\mathcal{K}_0$  and  $\mathcal{K}_1$  are positive constants and  $|\cdot|$  denotes the euclidean norm. We define the bilinear form  $B(\cdot, \cdot) : H_0^1(\Omega) \times H_0^1(\Omega) \rightarrow \mathbb{R}$  as the sum of three contributions, i.e.

$$B(u, v) := a(u, v) + b(u, v) + c(u, v), \quad \forall u, v \in H_0^1(\Omega), \quad (3)$$

where

$$a(u, v) := \int_{\Omega} (\mathcal{K} \nabla u) \cdot \nabla v, \quad (4)$$

$$b(u, v) := \int_{\Omega} (\beta \cdot \nabla u) v, \quad (5)$$

$$c(u, v) := \int_{\Omega} \gamma uv, \quad (6)$$

and, for the right-hand side, the linear form  $F(\cdot) : H_0^1(\Omega) \rightarrow \mathbb{R}$

$$F(v) := \int_{\Omega} f v \quad \forall v \in H_0^1(\Omega). \quad (7)$$

The variational formulation of (1) reads as: find  $u \in H_0^1(\Omega)$  such that,

$$B(u, v) = F(v) \quad \forall v \in H_0^1(\Omega). \quad (8)$$

More general boundary conditions can be considered and will be considered in the numerical tests.

## 3. Mesh and discretization

In order to define the discrete form of (8), let  $\mathcal{M}_h$  be a conforming polygonal tessellation of  $\Omega$  and  $E$  denotes a generic polygon of  $\mathcal{M}_h$ . Moreover, let  $h_E$  denote the diameter of  $E$  and the mesh size  $h := \max_{E \in \mathcal{M}_h} h_E$ .

We assume that  $\mathcal{M}_h$  satisfies the standard mesh assumptions for VEM, described in Assumption 3.1.

**Assumption 3.1** (Mesh assumptions).  $\exists \kappa > 0$  such that  $\forall E \in \mathcal{M}_h$ ,

- $E$  is star-shaped with respect to a ball of radius  $\rho_E \geq \kappa h_E$ ,
- for every edge  $e \subset \partial E$ ,  $|e| \geq \kappa h_E$ .

Notice that the above conditions imply that, denoting by  $N_E$  the number of vertices of  $E$ , it holds that the number of vertices of each polygon  $E$  has an upper bound, i.e.

$$\exists N_{\max} > 0 : \forall E \in \mathcal{M}_h, N_E \leq N_{\max}. \quad (9)$$

### 3.1. Discretization

Let  $\alpha = (\alpha_1, \alpha_2) \in \mathbb{N}^2$ , then we denote by  $\mathbf{x}^\alpha$  a generic element of degree  $|\alpha| = \alpha_1 + \alpha_2$  of the basis of homogeneous polynomials in  $\mathbb{R}^2$ , i.e.  $\mathbf{x}^\alpha = x_1^{\alpha_1} x_2^{\alpha_2}$ . For any given  $\omega \subset \mathbb{R}^2$ , let  $\mathbb{P}_k(\omega)$  be the space of polynomials of degree up to  $k$  defined on  $\omega$ , and given  $m, n \in \mathbb{N}$ , with  $n < m$ , let

$$\mathbb{P}_m(\omega) \setminus \mathbb{P}_{n-1}(\omega) := \text{span}\{\mathbf{x}_\omega^\alpha\}_{|\alpha|=n}^m.$$

Then, let  $\Pi_k^{\nabla, E} : H^1(E) \rightarrow \mathbb{P}_k(E)$  be the  $H^1$  orthogonal operator, defined up to a constant by the orthogonality condition:  $\forall u \in H^1(E)$ ,

$$\left(\nabla \left(\Pi_k^{\nabla, E} u - u\right), \nabla p\right)_E = 0 \quad \forall p \in \mathbb{P}_k(E). \tag{10}$$

In order to define  $\Pi_k^{\nabla, E}$  uniquely, we choose any continuous and linear projection operator  $P_0 : H^1(E) \rightarrow \mathbb{P}_0(E)$ , whose continuity constant in  $H^1$  norm is independent of  $h_E$  and continuous with respect to deformations of the geometry, and we impose  $\forall u \in H^1(E)$ ,

$$P_0\left(\Pi_k^{\nabla, E} u - u\right) = 0. \tag{11}$$

**Remark 1.** Under the current mesh assumptions, given by [Assumption 3.1](#), a suitable choice for  $P_0$  is the integral mean on  $E$ , i.e.

$$P_0(u) := \frac{1}{|E|} \int_E u \, dx \quad \forall u \in H^1(E).$$

Notice that this is a common choice, see for instance [\[2\]](#).

For any given  $E \in \mathcal{M}_h$ , we define the local Virtual Space of order  $k$  according to [\[2,26\]](#) as

$$\begin{aligned} \mathcal{V}_{h,k}^E &:= \{v_h \in H^1(E) : \Delta v_h \in \mathbb{P}_k(E), \gamma^e(v_h) \in \mathbb{P}_k(e) \forall e \subset \partial E, \\ v_h &\in C^0(\partial E), \left(v_h - \Pi_k^{\nabla, E} v_h, p\right)_E = 0 \forall p \in \mathbb{P}_k(E) \setminus \mathbb{P}_{k-2}(E)\} \end{aligned} \tag{12}$$

Given  $v_h \in \mathcal{V}_{h,k}^E$ , the chosen degrees of freedom of this space are

- $N_E$  pointwise values of  $v_h$  at the vertices of the polygon,
- if  $k > 1$ ,  $k - 1$  pointwise values of  $v_h$  at Gauss–Lobatto quadrature points internal to each edge,
- if  $k > 1$ ,  $\frac{k(k-1)}{2}$  internal moments  $\frac{1}{E}(v_h, m_i)_E, \forall i = 1, \dots, n_{k-2}$ , where  $n_{k-2} := \dim \mathbb{P}_{k-2}(E)$  and  $\{m_i\}_{i=1}^{n_{k-2}}$  is the scalar monomial basis of  $\mathbb{P}_{k-2}(E)$  defined as  $m_i := \left(\frac{\mathbf{x} - \mathbf{x}_E}{h_E}\right)^{\alpha_i}$ , correlating each index  $i$  to a multi-index  $\alpha_i = (\alpha_{i,1}, \alpha_{i,2})$  such that  $|\alpha_i| \leq k - 2$ .

Moreover, we define the global discrete space as  $\mathcal{V}_{h,k} := \{v \in H_0^1(\Omega) : v|_E \in \mathcal{V}_{h,k}^E\}$ . Note that  $v_h \in \mathcal{V}_{h,k}$  is a continuous function that is a polynomial of degree  $k$  on each edge of the mesh.

To define our discrete bilinear form, for any given  $E \in \mathcal{M}_h$ , let  $\ell_E$  be a given natural number and let  $\mathcal{P}_{k,\ell_E}(E)$  be the polynomial space given by

$$\begin{aligned} \mathcal{P}_{k,\ell_E} &:= \left[\mathbb{P}_{k-1}(E)\right]^2 \oplus \mathbf{curl} \left(\mathbb{P}_{k+\ell_E}(E) \setminus \mathbb{P}_k(E)\right) \\ &= \mathbf{x} \mathbb{P}_{k-2}(E) \oplus \mathbf{curl} \mathbb{P}_{k+\ell_E}(E), \end{aligned} \tag{13}$$

where for any  $p \in \mathbb{P}_{k+\ell_E}(E)$ ,  $\mathbf{curl} p = \left(\frac{\partial p}{\partial x_2}, -\frac{\partial p}{\partial x_1}\right)$ . Notice that  $\mathcal{P}_{k,\ell_E} \subset \left[\mathbb{P}_{k+\ell_E-1}(E)\right]^2$  and that we exploit the surjectivity of the divergence operator defined from  $\mathbf{x} \mathbb{P}_{k-2}(E)$  to  $\mathbb{P}_{k-2}(E)$  (see [\[27, Prop. 2.3.3\]](#)). Then, let  $\Pi_p^{0,E} \nabla : H^1(E) \rightarrow \mathcal{P}_{k,\ell_E}$  be the  $L^2$ -projection operator of the gradient of functions in  $H^1(E)$ , defined,  $\forall u \in H^1(E)$ , by the orthogonality condition

$$\left(\Pi_p^{0,E} \nabla u, p\right)_E = (\nabla u, p)_E \quad \forall p \in \mathcal{P}_{k,\ell_E}. \tag{14}$$

**Remark 2.** Notice that for each function  $u_h \in \mathcal{V}_{h,k}^E$ , the projection  $\Pi_p^{0,E} \nabla u_h$  is computable exploiting only the degrees of freedom of  $u_h$ .

Now, we can define the discrete bilinear forms. Let  $\mathcal{B}_h^E : \mathcal{V}_{h,k}^E \times \mathcal{V}_{h,k}^E \rightarrow \mathbb{R}$  be defined as

$$\mathcal{B}_h^E(u_h, v_h) := a_h^E(u_h, v_h) + b_h^E(u_h, v_h) + c_h^E(u_h, v_h) \quad \forall u_h, v_h \in \mathcal{V}_{h,k}^E, \tag{15}$$

and  $a_h^E, b_h^E, c_h^E : \mathcal{V}_{h,k}^E \times \mathcal{V}_{h,k}^E \rightarrow \mathbb{R}$  defined,  $\forall u_h, v_h \in \mathcal{V}_{h,k}^E$ , as

$$a_h^E(u_h, v_h) := \left(\mathcal{K} \cdot \Pi_p^{0,E} \nabla u_h, \Pi_p^{0,E} \nabla v_h\right)_E, \tag{16}$$

$$b_h^E(u_h, v_h) := (\beta \cdot \Pi_{k-1}^{0,E} \nabla u_h, \Pi_k^{0,E} v_h)_E, \tag{17}$$

$$c_h^E(u_h, v_h) := (\gamma \Pi_k^{0,E} u_h, \Pi_k^{0,E} v_h)_E. \tag{18}$$

where,  $\forall E \in \mathcal{M}_h$ ,  $\Pi_k^{0,E} : L^2(E) \rightarrow \mathbb{P}_k(E)$  is the  $L^2$ -projection, defined  $\forall u \in L^2(E)$  by

$$\left(\Pi_k^{0,E} u, p\right)_E = (u, p)_E \quad \forall p \in \mathbb{P}_k(E). \tag{19}$$

The above projection is computable for any given  $v_h \in \mathcal{V}_{h,k}$ . We remark that from the assumption on the diffusive tensor  $\mathcal{K}$  given in (2), for any  $E \in \mathcal{M}_h$ , we define:

$$\mathcal{K}_E^\vee := \inf_{x \in E} \sup_{v \in \mathbb{R}^2} \frac{v \cdot \mathcal{K}(x)v}{|v|^2}, \quad \mathcal{K}_E^\wedge := \sup_{x \in E} \sup_{v \in \mathbb{R}^2} \frac{v \cdot \mathcal{K}(x)v}{|v|^2}. \tag{20}$$

Summing up over all the elements of  $\mathcal{M}_h$ , we define  $B_h : \mathcal{V}_{h,k} \times \mathcal{V}_{h,k} \rightarrow \mathbb{R}$  as

$$B_h(u_h, v_h) := \sum_{E \in \mathcal{M}_h} B_h^E(u_h, v_h) \quad \forall u_h, v_h \in \mathcal{V}_{h,k}, \tag{21}$$

which results to be the sum of the following global discrete bilinear forms:

$$a_h(u_h, v_h) := \sum_{E \in \mathcal{M}_h} a_h^E(u_h, v_h) \tag{22}$$

$$b_h(u_h, v_h) := \sum_{E \in \mathcal{M}_h} b_h^E(u_h, v_h) \tag{23}$$

$$c_h(u_h, v_h) := \sum_{E \in \mathcal{M}_h} c_h^E(u_h, v_h) \tag{24}$$

We can state the discrete problem as: find  $u_h \in \mathcal{V}_{h,k,\varrho}$  such that

$$B_h(u_h, v_h) = \sum_{E \in \mathcal{M}_h} (f, \Pi_k^{0,E} v_h)_E \quad \forall v_h \in \mathcal{V}_{h,k}. \tag{25}$$

#### 4. Well-posedness

The main result presented in this section consists in the coercivity and continuity of the bilinear discrete form  $a_h^E$  defined in (16). In this perspective, we previously introduce the following notations. Let  $E \in \mathcal{M}_h$ ,  $\{\phi_i^\circ\}_{i=1}^{kN_E}$  denotes the set of basis functions of  $\mathcal{V}_{h,k}^E$  which are lagrangian with respect to the boundary degrees of freedom of  $\mathcal{V}_{h,k}^E$ , and the set of basis functions  $\{\phi_i^\circ\}_{i=1}^{n_{k-2}}$  of  $\mathcal{V}_{h,k}^E$  which are lagrangian with respect to the internal degrees of freedom of  $\mathcal{V}_{h,k}^E$ . Hence, let us consider the decomposition  $\mathcal{V}_{h,k}^E = \mathcal{V}_k^\circ(E) \oplus \mathcal{V}_k^\partial(E)$ , where  $\mathcal{V}_k^\circ(E) = \text{span}\{\phi_i^\circ, \forall i = 1, \dots, n_{k-2}\}$  and  $\mathcal{V}_k^\partial(E) = \text{span}\{\phi_i^\partial, \forall i = 1, \dots, kN_E\}$ . For each  $u_h \in \mathcal{V}_{h,k}^E$ , there exist unique  $u_h^\circ \in \mathcal{V}_k^\circ(E)$  and  $u_h^\partial \in \mathcal{V}_k^\partial(E)$  such that  $u_h = u_h^\circ + u_h^\partial$  and  $u_h^\circ = \sum_{i=1}^{n_{k-2}} \lambda_i^\circ(u_h^\circ) \phi_i^\circ$  and  $u_h^\partial = \sum_{i=1}^{kN_E} \lambda_i^\partial(u_h^\partial) \phi_i^\partial$ . In the following, we omit the dependency of  $\lambda_i^\circ$  and  $\lambda_i^\partial$  on the virtual function, with a slight abuse of notation.

Furthermore, without loss of generality let  $\{\pi_i\}_{i=1}^{kN_E-1}$  denote a set of scaled basis functions of the space  $\mathbb{P}_{k-1}^0(\partial E) := \{\pi : \pi|_e \in \mathbb{P}_{k-1}(e), \forall e \subset \partial E, \int_{\partial E} \pi = 0\}$ , such that  $\|\pi_i\|_{L^\infty(\partial E)} = 1$ . Hence for a given  $u_h^\partial \in \mathcal{V}_k^\partial(E)$ , since the tangential derivative  $\nabla u_h^\partial \cdot t|_{\partial E} \in \mathbb{P}_{k-1}^0(\partial E)$  let  $\Lambda_i^\partial(u_h^\partial)$  be defined such that

$$\nabla u_h^\partial \cdot t|_{\partial E} = \sum_{i=1}^{kN_E-1} \Lambda_i^\partial(u_h^\partial) \pi_i. \tag{26}$$

In the following, we omit the dependency of  $\Lambda_i^\partial$  on the virtual function, with a slight abuse of notation.

**Lemma 1.** *Let  $E \in \mathcal{M}_h$  and let  $u_h^\partial \in \mathcal{V}_k^\partial(E)$ . Then, the following estimates hold true:*

$$C^\partial \|\nabla u_h^\partial\|_{L^2(E)} \leq \sqrt{h_E |\partial E|} \sum_{i=1}^{kN_E-1} |\Lambda_i^\partial|, \tag{27}$$

$$\frac{C^\partial}{kN_E - 1} \|\nabla u_h^\partial\|_{L^2(E)} \leq \sqrt{h_E |\partial E|} \max_i |\Lambda_i^\partial|, \tag{28}$$

for a positive constant  $C^\partial$  independent of  $h_E$  and depending on the ratio  $\rho_E/h_E$ .

**Proof.** First, let us recall the following result that can be proved following the techniques in [28, Proposition 4.4] and in [29, Lemma 3.19]. For any  $u_h^\partial \in \mathcal{V}_k^\partial(E)$ , the estimate

$$C^\partial \|\nabla u_h^\partial\|_{L^2(E)} \leq h_E^{\frac{1}{2}} \|\nabla u_h^\partial \cdot t\|_{L^2(\partial E)},$$

holds for a positive constant  $C^\partial$  depending only on the ratio  $\rho_E/h_E$ . Hence, the norm at the right-hand side can be estimated as follows:

$$\begin{aligned} (C^\partial)^2 \left\| \nabla u_h^\partial \right\|_{L^2(E)}^2 &\leq h_E \left\| \nabla u_h^\partial \cdot \boldsymbol{t} \right\|_{L^2(\partial E)}^2 \\ &= h_E \sum_{i=1}^{kN_E-1} (\Lambda_i^\partial)^2 \int_{\partial E} \pi_i^2 ds \leq h_E |\partial E| \sum_{i=1}^{kN_E-1} (\Lambda_i^\partial)^2, \end{aligned}$$

which yields (27). The estimate (28) derives immediately from (27), since

$$\sum_{i=1}^{kN_E-1} \left| \Lambda_i^\partial (u_h^\partial) \right| \leq (kN_E - 1) \max_i \left| \Lambda_i^\partial \right|. \quad \square$$

**Lemma 2.** Under the mesh Assumption 3.1, for every  $E \in \mathcal{M}_h$  and for every  $u_h^\circ \in \mathcal{V}_k^\circ(E) \exists \boldsymbol{p}_*^\circ \in \mathbf{x}^{\mathbb{P}_{k-2}}(E)$  such that

$$(\nabla u_h^\circ, \boldsymbol{p}_*^\circ) \geq C^\circ \left\| \nabla u_h^\circ \right\|_{L^2(E)}, \tag{29}$$

$$\left\| \boldsymbol{p}_*^\circ \right\|_{L^2(E)} \leq \overline{C}^\circ, \tag{30}$$

where  $C^\circ$  and  $\overline{C}^\circ$  are two positive constants independent of  $h_E$ .

**Proof.** Recalling that  $u_h^\circ = \sum_{i=1}^{n_{k-2}} \lambda_i^\circ \phi_i^\circ$ , we define  $\boldsymbol{p}_*^\circ \in \mathbf{x}^{\mathbb{P}_{k-2}}(E)$  as

$$\boldsymbol{p}_*^\circ := \sum_{i=1}^{n_{k-2}} \frac{sg(\lambda_i^\circ)}{|E|} \mathbf{m}_i \tag{31}$$

where for each  $i = 1, \dots, n_{k-2}$  and  $m_i$  scaled monomial basis function of  $\mathbb{P}_{k-2}(E)$ , i.e.  $m_i = m_{(\alpha_{i,1}, \alpha_{i,2})} = \left(\frac{x_1 - x_{E,1}}{h_E}\right)^{\alpha_{i,1}} \left(\frac{x_2 - x_{E,2}}{h_E}\right)^{\alpha_{i,2}}$ ,  $\mathbf{m}_i$  is given by

$$\mathbf{m}_i = -\frac{h_E}{\alpha_{i,1} + \alpha_{i,2} + 2} \begin{pmatrix} m_{(\alpha_{i,1}+1, \alpha_{i,2})} \\ m_{(\alpha_{i,1}, \alpha_{i,2}+1)} \end{pmatrix}.$$

Notice that  $\mathbf{m}_i$  satisfies  $-\nabla \cdot \mathbf{m}_i = m_i$ . Hence, exploiting the definition of the internal degrees of freedom and the equivalence of norms we obtain

$$\begin{aligned} (\nabla u_h^\circ, \boldsymbol{p}_*^\circ)_E &= - (u_h^\circ, \nabla \cdot \boldsymbol{p}_*^\circ)_E = \sum_{i=1}^{n_{k-2}} \frac{sg(\lambda_i^\circ)}{|E|} (u_h^\circ, m_i)_E \\ &= \sum_{i=1}^{n_{k-2}} sg(\lambda_i^\circ) \lambda_i^\circ = \sum_{i=1}^{n_{k-2}} |\lambda_i^\circ| \geq C^\circ \left\| \nabla u_h^\circ \right\|_{L^2(E)}, \end{aligned}$$

which proves (29). On the other hand, using the definition (31), Young’s inequality and since  $\left\| m_{(\alpha_{i,1}, \alpha_{i,2})} \right\|_{L^\infty(E)} \leq 1 \forall i$ , we get (30) as follows

$$\begin{aligned} \left\| \boldsymbol{p}_*^\circ \right\|_{L^2(E)}^2 &= \frac{1}{|E|^2} \sum_{i=1}^{n_{k-2}} \sum_{j=1}^{n_{k-2}} \int_E \mathbf{m}_i \cdot \mathbf{m}_j \leq \frac{n_{k-2}}{2|E|^2} \sum_{i=1}^{n_{k-2}} \left\| \mathbf{m}_i \right\|_{L^2(E)}^2 \\ &= \frac{n_{k-2}}{2|E|^2} \sum_{i=1}^{n_{k-2}} \frac{h_E^2}{(\alpha_{i,1} + \alpha_{i,2} + 2)^2} \int_E \left( m_{(\alpha_{i,1}+1, \alpha_{i,2})}^2 + m_{(\alpha_{i,1}, \alpha_{i,2}+1)}^2 \right) \\ &= \frac{n_{k-2}}{|E|} \sum_{i=1}^{n_{k-2}} \frac{h_E^2}{(\alpha_{i,1} + \alpha_{i,2} + 2)^2} = \frac{n_{k-2} h_E^2}{|E|} \sum_{j=0}^{k-2} \frac{j+1}{(j+2)^2} =: \overline{C}^{\circ 2}, \end{aligned}$$

where at the last step we used the fact that there exactly  $j + 1$  monomials of degree  $j$ . Notice that  $\overline{C}^\circ$  depends on  $k$  and the polygon regularity parameter, but it does not depend on  $h_E$ .  $\square$

As a further ingredient, the proof of the local coercivity requires an assumption on  $\ell_E$ .

**Assumption 4.1.** We assume  $\ell_E$  to be the smallest integer such that any polynomial  $q \in \mathbb{P}_{k+\ell_E}(E)$  can be identified by a set of degrees of freedom which contains  $kN_E - 1$  distinct moments  $\frac{1}{|\partial E|} (q, \pi_i)_{\partial E}$  with respect to a scaled polynomial basis of the space  $\mathbb{P}_{k-1}^0(\partial E) := \{\pi : \pi|_e \in \mathbb{P}_{k-1}(e), \forall e \subset \partial E, \int_{\partial E} \pi = 0\}$ .

**Remark 3.** Assumption 4.1 is equivalent to assert that the  $L^2(\partial E)$ -orthogonal projection operator defined from  $\mathbb{P}_{k+\ell_E}(E)$  to  $\mathbb{P}_{k-1}^0(\partial E)$  is surjective.

**Theorem 1.** Under the mesh Assumptions 3.1 and 4.1, for every  $E \in \mathcal{M}_h$ , the projection operator  $\Pi_P^{0,E} \nabla$ , defined in (14), is coercive, namely there exists a positive constant  $\alpha_*^E$ , independent of  $h_E$ , such that

$$\left\| \Pi_P^{0,E} \nabla u_h \right\|_{L^2(E)}^2 \geq \alpha_*^E \left\| \nabla u_h \right\|_{L^2(E)}^2, \quad \forall u_h \in \mathcal{V}_{h,k}^E. \tag{32}$$

**Proof.** From the definition of the operator  $\Pi_P^{0,E} \nabla$  (14), we have

$$\frac{\left\| \Pi_P^{0,E} \nabla u_h \right\|_{L^2(E)}}{\left\| \nabla u_h \right\|_{L^2(E)}} = \sup_{p \in \mathcal{P}_{k,\ell}} \frac{\left( \Pi_P^{0,E} \nabla u_h, p \right)_E}{\left\| \nabla u_h \right\|_{L^2(E)} \left\| p \right\|_{L^2(E)}} = \sup_{p \in \mathcal{P}_{k,\ell}} \frac{\left( \nabla u_h, p \right)_E}{\left\| \nabla u_h \right\|_{L^2(E)} \left\| p \right\|_{L^2(E)}}. \tag{33}$$

We now consider  $u_h = u_h^\circ + u_h^\partial$ , with  $u_h^\circ \in \mathcal{V}_k^\circ(E)$  and  $u_h^\partial \in \mathcal{V}_k^\partial(E)$ , and we employ Lemma 2 denoting by  $p_*^\circ \in \mathbf{x}\mathbb{P}_{k-2}^\circ(E)$  the polynomial that satisfies (29) and (30). Let  $p_*^\partial \in \mathbf{curl}\mathbb{P}_{k+\ell_E}^\partial(E)$  such that  $p_* := p_*^\partial + p_*^\circ$ , then (33) can be rewritten as

$$\begin{aligned} \frac{\left\| \Pi_P^{0,E} \nabla u_h \right\|_{L^2(E)}}{\left\| \nabla u_h \right\|_{L^2(E)}} &\geq \frac{\left( \nabla u_h^\circ, p_* \right)_E + \left( \nabla u_h^\partial, p_* \right)_E}{\left\| \nabla u_h \right\|_{L^2(E)} \left\| p_* \right\|_{L^2(E)}} = \frac{\left( \nabla u_h^\circ, p_*^\circ \right)_E + \left( \nabla u_h^\partial, p_* \right)_E}{\left\| \nabla u_h \right\|_{L^2(E)} \left\| p_* \right\|_{L^2(E)}} \\ &\geq \frac{C^\circ \left\| \nabla u_h^\circ \right\|_{L^2(E)} + \left( \nabla u_h^\partial, p_* \right)_E}{\left\| \nabla u_h \right\|_{L^2(E)} \left( \left\| p_*^\partial \right\|_{L^2(E)} + \overline{C^\circ} \right)}. \end{aligned} \tag{34}$$

Let us focus on the term at the numerator of (34)

$$\left( \nabla u_h^\partial, p_* \right)_E = \left( \nabla u_h^\partial, p_*^\partial \right)_E + \left( \nabla u_h^\partial, p_*^\circ \right)_E. \tag{35}$$

Let  $q \in \mathbb{P}_{k+\ell_E}^\partial(E)$  be such that  $p_*^\partial = \mathbf{curl} q$ , hence we have

$$\left( \nabla u_h^\partial, p_*^\partial \right)_E = \left( \nabla u_h^\partial, \mathbf{curl} q \right)_E = \left( \nabla u_h^\partial \cdot t, q \right)_{\partial E}, \tag{36}$$

where  $q \in \mathbb{P}_{k+\ell_E}^\partial(\partial E)$  represents the trace of the polynomial  $q$  on  $\partial E$  when no confusion arises.

Applying the representation of  $\nabla u_h^\partial \cdot t$  given in (26), let  $\Lambda_{i_M}^\partial$  be the maximum of  $\{\Lambda_i^\partial\}_{i=1}^{kN_E-1}$ , and, by using Lemma 1, it holds true that

$$\sqrt{h_E} |\partial E| \Lambda_{i_M}^\partial := \sqrt{h_E} |\partial E| \max_i |\Lambda_i^\partial| \geq \frac{C^\partial}{kN_E - 1} \left\| \nabla u_h^\partial \right\|_{L^2(E)}. \tag{37}$$

We now employ the key Assumption 4.1 by setting the moments of  $q$  with respect of each basis function  $\{\pi_i\}_{i=1}^{kN_E-1}$  as follows

$$\begin{aligned} \frac{1}{|\partial E|} \left( q, \pi_{i_M} \right)_{\partial E} &:= sg(\Lambda_{i_M}^\partial) \frac{\sqrt{h_E} |\partial E|}{|\partial E|} - \frac{\left( \nabla u_h^\partial, p_*^\circ \right)_E}{\Lambda_{i_M}^\partial} \frac{1}{|\partial E|}, \\ \frac{1}{|\partial E|} \left( q, \pi_i \right)_{\partial E} &:= sg(\Lambda_i^\partial) \frac{\sqrt{h_E} |\partial E|}{|\partial E|}, \end{aligned} \quad \forall i \neq i_M,$$

and all the other degrees of freedom of  $q$  eventually present are set to zero. Substituting these definitions of the moments of  $q$  in (35), and using Lemma 1

$$\left( \nabla u_h^\partial, p_* \right)_E = \sqrt{h_E} |\partial E| \sum_{i=1}^{kN_E-1} |\Lambda_i^\partial| \geq C^\partial \left\| \nabla u_h^\partial \right\|_{L^2(E)}. \tag{38}$$

On the other hand, we remark that from (30) and (37) we get

$$\left| \frac{\left( \nabla u_h^\partial, p_*^\circ \right)_E}{\Lambda_{i_M}^\partial |\partial E|} \right| \leq \frac{\sqrt{h_E} |\partial E| (kN_E - 1) \left\| \nabla u_h^\partial \right\|_{L^2(E)} \left\| p_*^\circ \right\|_{L^2(E)}}{C^\partial |\partial E| \left\| \nabla u_h^\partial \right\|_{L^2(E)}} \leq \frac{\sqrt{h_E} |\partial E|}{|\partial E|} (kN_E - 1) \frac{\overline{C^\circ}}{C^\partial},$$

and employing the definitions of the moments of  $q$  and we obtain, by a scaling argument,

$$\left\| p_*^\partial \right\|_{L^2(E)} = \left\| \mathbf{curl} q \right\|_{L^2(E)} \leq C_{eq} \left( \left| \frac{\left( \nabla u_h^\partial, p_*^\circ \right)_E}{\Lambda_{i_M}^\partial |\partial E|} \right| + \sum_{i=1}^{kN_E-1} \frac{\sqrt{h_E} |\partial E|}{|\partial E|} \right) \leq \overline{C^\partial}, \tag{39}$$

where  $C_{eq}$  and  $\overline{C^\partial}$  are positive constants independent of  $h_E$ . In particular,  $C_{eq} := \max_i \left\| \nabla \psi_i \right\|_{L^2(E)}$ , where  $\{\psi_i\}_i$  is a set of basis function of  $\mathbb{P}_{k+\ell_E}^\partial(E)$  Lagrangian in the degrees of freedom defined in Assumption 4.1. With the two bounds (38) and (39) at hand, we can conclude the proof by replacing them in (34)

$$\frac{\left\| \Pi_P^{0,E} \nabla u_h \right\|_{L^2(E)}}{\left\| \nabla u_h \right\|_{L^2(E)}} \geq \frac{C^\circ \left\| \nabla u_h^\circ \right\|_{L^2(E)} + C^\partial \left\| \nabla u_h^\partial \right\|_{L^2(E)}}{\left\| \nabla u_h \right\|_{L^2(E)} \left( \overline{C^\circ} + \overline{C^\partial} \right)} \geq \frac{\min\{C^\circ, C^\partial\}}{\overline{C^\circ} + \overline{C^\partial}} =: \alpha_*^E,$$

where we use the triangle inequality  $\left\| \nabla u_h \right\|_{L^2(E)} \leq \left\| \nabla u_h^\circ \right\|_{L^2(E)} + \left\| \nabla u_h^\partial \right\|_{L^2(E)}$ .  $\square$

Now, for each  $E \in \mathcal{M}_h$ , let

$$\|u_h\|_E^2 := \|\sqrt{\mathcal{K}} \nabla u_h\|_{L^2(E)}^2 + \|\sqrt{\gamma} \Pi_k^0 u_h\|_{L^2(E)}^2, \quad \forall u_h \in \mathcal{V}_{h,k}^E.$$

Furthermore, we define the respective global norm as

$$\|u_h\|_\Omega^2 := \sum_{E \in \mathcal{M}_h} \|u_h\|_E^2, \quad \forall u_h \in \mathcal{V}_{h,k}.$$

**Theorem 2.** Under the mesh Assumptions 3.1 and 4.1, the bilinear form  $B_h$ , defined in (21), is continuous, i.e. there exists a positive constant  $\Xi^*$  such that

$$B_h(u_h, v_h) \leq \Xi^* \|u_h\|_\Omega \|v_h\|_\Omega, \quad \forall u_h, v_h \in \mathcal{V}_{h,k}. \tag{40}$$

**Proof.** For every  $u_h, v_h \in \mathcal{V}_{h,k}$ , employing the definition of the bilinear form  $a_h$  (22) and the continuity of the projection operator  $\Pi_p^{0,E} \nabla$  (14), the Cauchy–Schwarz inequality, and the hypothesis on  $\mathcal{K}$  (2) and (20), we get

$$\begin{aligned} a_h(u_h, v_h) &= \sum_{E \in \mathcal{M}_h} a_h^E(u_h, v_h) \\ &= \sum_{E \in \mathcal{M}_h} \left( \mathcal{K} \Pi_p^{0,E} \nabla u_h, \Pi_p^{0,E} \nabla v_h \right)_E \leq \sum_{E \in \mathcal{M}_h} \mathcal{K}_E^\wedge \left( \nabla u_h, \Pi_p^{0,E} \nabla v_h \right)_E \\ &\leq \sum_{E \in \mathcal{M}_h} \mathcal{K}_E^\wedge \|\nabla u_h\|_{L^2(E)} \|\Pi_p^{0,E} \nabla v_h\|_{L^2(E)} \leq \sum_{E \in \mathcal{M}_h} \mathcal{K}_E^\wedge \|\nabla u_h\|_{L^2(E)} \|\nabla v_h\|_{L^2(E)} \\ &\leq \sum_{E \in \mathcal{M}_h} \frac{\mathcal{K}_E^\wedge}{\mathcal{K}_E^\vee} \|\sqrt{\mathcal{K}} \nabla u_h\|_{L^2(E)} \|\sqrt{\mathcal{K}} \nabla v_h\|_{L^2(E)}. \end{aligned} \tag{41}$$

On the other hand, for the bilinear forms  $b_h$  (23), we employ the continuity of operator  $\Pi_{k-1}^{0,E}$  and the Poincaré inequality on  $\Omega$ . In particular, we get

$$\begin{aligned} |b_h(u_h, v_h)| &\leq \sum_{E \in \mathcal{M}_h} |b_h^E(u_h, v_h)| = \sum_{E \in \mathcal{M}_h} \left| \left( \beta \cdot \Pi_{k-1}^{0,E} \nabla u_h, \Pi_k^{0,E} v_h \right)_E \right| \\ &\leq \sum_{E \in \mathcal{M}_h} \|\beta\|_{L^\infty(E)} \|\Pi_{k-1}^{0,E} \nabla u_h\|_{L^2(E)} \|\Pi_k^{0,E} v_h\|_{L^2(E)} \\ &\leq \sum_{E \in \mathcal{M}_h} \|\beta\|_{L^\infty(E)} \|\nabla u_h\|_{L^2(E)} \|v_h\|_{L^2(E)} \\ &\leq \max_{E \in \mathcal{M}_h} \left( \frac{\|\beta\|_{L^\infty(E)}}{\sqrt{\mathcal{K}_E^\vee}} \right) \sum_{E \in \mathcal{M}_h} \|\sqrt{\mathcal{K}} \nabla u_h\|_{L^2(E)} \|v_h\|_{L^2(E)} \\ &\leq \max_{E \in \mathcal{M}_h} \left( \frac{\|\beta\|_{L^\infty(E)}}{\sqrt{\mathcal{K}_E^\vee}} \right) \|\sqrt{\mathcal{K}} \nabla u_h\|_{L^2(\Omega)} \|v_h\|_{L^2(\Omega)} \\ &\leq C_P h \max_{E \in \mathcal{M}_h} \left( \frac{\|\beta\|_{L^\infty(E)}}{\sqrt{\mathcal{K}_E^\vee}} \right) \|\sqrt{\mathcal{K}} \nabla u_h\|_{L^2(\Omega)} \|\nabla v_h\|_{L^2(\Omega)} \\ &\leq C_P h \max_{E \in \mathcal{M}_h} \left( \frac{\|\beta\|_{L^\infty(E)}}{\sqrt{\mathcal{K}_E^\vee}} \right) \max_{E \in \mathcal{M}_h} \frac{1}{\sqrt{\mathcal{K}_E^\vee}} \|\sqrt{\mathcal{K}} \nabla u_h\|_{L^2(\Omega)} \|\sqrt{\mathcal{K}} \nabla v_h\|_{L^2(\Omega)}. \end{aligned} \tag{42}$$

Finally, for the bilinear form  $c_h$  (24) we have that

$$\begin{aligned} c_h(u_h, v_h) &= \sum_{E \in \mathcal{M}_h} c_h^E(u_h, v_h) = \sum_{E \in \mathcal{M}_h} \left( \gamma \Pi_k^{0,E} u_h, \Pi_k^{0,E} v_h \right)_E \\ &= \sum_{E \in \mathcal{M}_h} \left( \sqrt{\gamma} \Pi_k^{0,E} u_h, \sqrt{\gamma} \Pi_k^{0,E} v_h \right)_E \\ &= \sum_{E \in \mathcal{M}_h} \|\sqrt{\gamma} \Pi_k^{0,E} u_h\|_{L^2(E)} \|\sqrt{\gamma} \Pi_k^{0,E} v_h\|_{L^2(E)}. \end{aligned} \tag{43}$$

Recalling the definition of the bilinear for (21), summing up (41), (42), and (43), we conclude the proof.  $\square$

**Theorem 3.** For a sufficient small  $h$ , and under the mesh Assumptions 3.1 and 4.1, the bilinear form  $B_h$ , defined in (21), is coercive, i.e. there exists a positive constant  $\Xi_*$  such that

$$B_h(u_h, u_h) \geq \Xi_* \|u_h\|_{L^2(\Omega)}^2, \quad \forall u_h \in \mathcal{V}_{h,k}. \tag{44}$$

**Proof.** Let  $u_h \in \mathcal{V}_{h,k}$ , from the definition of  $a_h^E$  (16), employing Theorem 1 and the definitions of  $\mathcal{K}_E^\vee$  and  $\mathcal{K}_E^\wedge$  (20), we get

$$\begin{aligned} a_h(u_h, u_h) &= \sum_{E \in \mathcal{M}_h} a_h^E(u_h, u_h) = \sum_{E \in \mathcal{M}_h} \left( \mathcal{K} \Pi_p^{0,E} \nabla u_h, \Pi_p^{0,E} \nabla u_h \right)_E \\ &\geq \sum_{E \in \mathcal{M}_h} \mathcal{K}_E^\vee \left\| \Pi_p^{0,E} \nabla u_h \right\|_{L^2(E)}^2 \geq \sum_{E \in \mathcal{M}_h} \mathcal{K}_E^\vee \alpha_*^E \left\| \nabla u_h \right\|_{L^2(E)}^2 \geq \sum_{E \in \mathcal{M}_h} \frac{\mathcal{K}_E^\vee}{\mathcal{K}_E^\wedge} \alpha_*^E \left\| \sqrt{\mathcal{K}} \nabla u_h \right\|_{L^2(E)}^2. \end{aligned}$$

On the other hand, given the definition of  $b_h$  (5), using the continuity of the bilinear form (42), we have

$$b_h(u_h, u_h) \geq -C_p h \max_{E \in \mathcal{M}_h} \left( \frac{\|\beta\|_{L^\infty(E)}}{\sqrt{\mathcal{K}_E^\vee}} \right) \max_{E \in \mathcal{M}_h} \frac{1}{\sqrt{\mathcal{K}_E^\vee}} \left\| \sqrt{\mathcal{K}} \nabla u_h \right\|_{L^2(\Omega)}^2$$

where  $C_p$  is the Poincaré constant. Finally, for the reactive term  $c_h$  (6), we proceed as follows

$$c_h(u_h, u_h) = \sum_{E \in \mathcal{M}_h} c_h^E(u_h, u_h) = \sum_{E \in \mathcal{M}_h} \left( \gamma \Pi_k^{0,E} u_h, \Pi_k^{0,E} u_h \right)_E = \sum_{E \in \mathcal{M}_h} \left\| \sqrt{\gamma} \Pi_k^{0,E} u_h \right\|_{L^2(E)}^2.$$

We conclude the proof by summing the three global bilinear form and under the hypothesis that  $h$  is sufficiently small. In particular if for instance  $h$  is such that

$$C_p h \max_{E \in \mathcal{M}_h} \left( \frac{\|\beta\|_{L^\infty(E)}}{\mathcal{K}_E^\vee} \right) \max_{E \in \mathcal{M}_h} \sqrt{\frac{\mathcal{K}_E^\vee}{\mathcal{K}_0}} \leq \frac{1}{2} \min_{E \in \mathcal{M}_h} \frac{\mathcal{K}_E^\vee}{\mathcal{K}_E^\wedge} \alpha_*^E \tag{45}$$

it results  $\Xi_* = \min \left\{ 1, \frac{1}{2} \min_{E \in \mathcal{M}_h} \frac{\mathcal{K}_E^\vee}{\mathcal{K}_E^\wedge} \alpha_*^E \right\}$ .  $\square$

**Remark 4.** The assumption that  $h$  has to be sufficiently small is needed only if the bilinear form  $b_h$  is included in the operator  $B_h$ . Since we impose Dirichlet boundary conditions, we can overcome this assumption resorting to a skew-symmetric bilinear form  $b_h$  (see [4,30]). However, the extension to more general boundary conditions would not be straightforward.

This theorem implies that the bilinear form of the discrete problem (25) satisfies the hypothesis of the Lax–Milgram theorem, hence the problem admits a unique solution.

#### 4.1. Necessity of Assumption 4.1

In this subsection, we analyze Assumption 4.1. In particular, we prove that it is not only a sufficient but also a necessary condition, to get the coercivity of operator  $\Pi_p^{0,E} \nabla$  given in Theorem 1.

**Lemma 3.** Let  $\mathcal{V}_k^{\partial,0}(E) := \{v_h \in \mathcal{V}_k^\partial(E) : \int_{\partial E} v_h = 0\}$ . Then,

$$\forall \pi \in \mathbb{P}_{k-1}^0(\partial E), \exists ! u_h \in \mathcal{V}_k^{\partial,0}(E) : \pi = (\nabla u_h \cdot \mathbf{t})|_{\partial E}. \tag{46}$$

**Proof.** First, we notice that  $\dim(\mathbb{P}_{k-1}^0(\partial E)) = \dim(\mathcal{V}_k^{\partial,0}(E)) = kN_E - 1$  and  $\forall u_h \in \mathcal{V}_k^{\partial,0}(E), (\nabla u_h \cdot \mathbf{t})|_{\partial E} \in \mathbb{P}_{k-1}^0(\partial E)$ . Then, to prove (46) it is enough to show that, given a basis  $\{\varphi_i^\partial\}_{i=1}^{kN_E-1}$  of  $\mathcal{V}_k^{\partial,0}(E)$ , the set of functions  $\left\{ (\nabla \varphi_i^\partial \cdot \mathbf{t})|_{\partial E} \right\}_{i=1}^{kN_E-1}$  is linearly independent on  $\partial E$ . Suppose  $\exists \alpha_i, i = 1, \dots, kN_E - 1$  such that:

$$\sum_{i=1}^{kN_E-1} \alpha_i (\nabla \varphi_i^\partial \cdot \mathbf{t})|_{\partial E} = 0,$$

then, we get

$$\left( \nabla \left( \sum_{i=1}^{kN_E-1} \alpha_i \varphi_i^\partial \right) \cdot \mathbf{t} \right) \Big|_{\partial E} = 0.$$

Since  $\varphi_i^\partial \in C^0(\partial E)$ , there exists a constant  $c \in \mathbb{R}$ , such that

$$\left( \sum_{i=1}^{kN_E-1} \alpha_i \varphi_i^\partial \right) \Big|_{\partial E} = c.$$

Integrating on  $\partial E$ , and recalling that  $\int_{\partial E} \varphi_i^\partial = 0 \ \forall i = 1, \dots, kN_E - 1$ , we get that  $c = 0$ . Finally, since  $\{\varphi_i^\partial\}_{i=1}^{kN_E-1}$  form a basis of  $\mathcal{V}_k^{\partial,0}(E)$ , we conclude the proof.  $\square$

**Remark 5.** The space of the tangential derivatives of functions in  $\mathcal{V}_{h,k}$  is  $\mathbb{P}_{k-1}^0(\partial E)$ .

**Theorem 4.** Let  $E \in \mathcal{M}_h$  be given and let (32) hold true. Then Assumption 4.1 holds true.

**Proof.** To prove Assumption 4.1, we prove that the  $L^2(\partial E)$ -orthogonal projection on  $\mathbb{P}_{k-1}^0(\partial E)$ , denoted by  $\Pi_{k-1}^{0,\partial E}$ , is surjective from  $\mathbb{P}_{k+\ell_E}^{0,\partial E}(E)$  (see Remark 3). Consider the following subspace of  $\mathbb{P}_{k+\ell_E}(E)$ :

$$D_{k+\ell_E} := \left\{ p \in \mathbb{P}_{k+\ell_E}(E) : \mathbf{curl} p = \Pi_p^{0,E} \nabla v_h, \text{ for some } v_h \in \mathcal{V}_{h,k}^E, \int_{\partial E} p = 0 \right\}.$$

By (32) we have that  $\dim \text{Im} \Pi_p^{0,E} \nabla = kN_E + \frac{k(k-1)}{2} - 1$ . Then, since  $\forall u_h \in \mathcal{V}_{h,k}^E, \Pi_p^{0,E} \nabla u_h \in \mathbf{x} \mathbb{P}_{k-2}(E) \oplus \mathbf{curl} D_{k+\ell_E}$ ,

$$\dim D_{k+\ell_E} = \dim \text{Im} \Pi_p^{0,E} \nabla - \dim \mathbf{x} \mathbb{P}_{k-2}(E) = kN_E - 1 = \dim \mathbb{P}_{k-1}^0(\partial E). \tag{47}$$

Let  $\bar{p} \in D_{k+\ell_E}$ , and let  $\bar{v}_h \in \mathcal{V}_{h,k}^E$  such that  $\mathbf{curl} \bar{p} = \Pi_p^{0,E} \nabla \bar{v}_h$ , from Lemma 3 we have

$$\begin{aligned} \left\| \Pi_{k-1}^{0,\partial E} \bar{p} \right\|_{L^2(\partial E)} &= \sup_{\pi \in \mathbb{P}_{k-1}^0(\partial E)} \frac{(\pi, \bar{p})_{\partial E}}{\|\pi\|_{L^2(\partial E)}} = \sup_{u_h \in \mathcal{V}_{h,k}^E} \frac{(\nabla u_h \cdot \mathbf{t}, \bar{p})_{\partial E}}{\|\nabla u_h \cdot \mathbf{t}\|_{L^2(\partial E)}} \\ &\geq \frac{(\nabla \bar{v}_h \cdot \mathbf{t}, \bar{p})_{\partial E}}{\|\nabla \bar{v}_h \cdot \mathbf{t}\|_{L^2(\partial E)}} = \frac{(\nabla \bar{v}_h, \mathbf{curl} \bar{p})_{\partial E}}{\|\nabla \bar{v}_h \cdot \mathbf{t}\|_{L^2(\partial E)}} = \frac{\left\| \Pi_p^{0,E} \nabla \bar{v}_h \right\|_{L^2(E)}^2}{\|\nabla \bar{v}_h \cdot \mathbf{t}\|_{L^2(\partial E)}} \\ &= \frac{\left\| \Pi_p^{0,E} \nabla \bar{v}_h \right\|_{L^2(E)} \|\mathbf{curl} \bar{p}\|_{L^2(E)}}{\|\nabla \bar{v}_h \cdot \mathbf{t}\|_{L^2(\partial E)}} \geq \sqrt{\alpha_*^E} \frac{\|\nabla \bar{v}_h\|_{L^2(E)} \|\mathbf{curl} \bar{p}\|_{L^2(E)}}{\|\nabla \bar{v}_h \cdot \mathbf{t}\|_{L^2(\partial E)}}, \end{aligned}$$

where in the last step we have used (32). Finally, by using a trace inequality we get the injectivity of the operator. Indeed

$$\begin{aligned} \left\| \Pi_{k-1}^{0,\partial E} \bar{p} \right\|_{L^2(\partial E)} &\geq C \sqrt{\alpha_*^E} \frac{\|\nabla \bar{v}_h\|_{L^2(E)} \|\mathbf{curl} \bar{p}\|_{L^2(E)}}{h_E^{-1/2} \|\nabla \bar{v}_h\|_{L^2(E)}} \geq C \sqrt{\alpha_*^E} h_E^{1/2} \|\mathbf{curl} \bar{p}\|_{L^2(E)} \\ &\geq C \sqrt{\alpha_*^E} h_E^{-1/2} \|\bar{p}\|_{L^2(E)}, \end{aligned}$$

where the last equality holds since  $\int_{\partial E} \bar{p} = 0$ . By (47), we infer that the operator  $\Pi_{k-1}^{0,\partial E}$  is a bijection from  $D_{k+\ell_E}$  to  $\mathbb{P}_{k-1}^0(\partial E)$ , and is thus surjective from  $\mathbb{P}_{k+\ell_E}^{0,\partial E}(E)$ . Thus, Assumption 4.1 is satisfied.  $\square$

To conclude, the proof of Theorem 4 implies that Assumption 4.1 and (32) are equivalent.

### 5. Error estimates

In this section, we derive optimal a priori error estimates for the proposed scheme. First, we need to recall well-known results in literature about polynomial approximation and interpolation error estimates for the VEM space  $\mathcal{V}_{h,k}$  (see [31, Theorem 11]).

**Lemma 4.** Under Assumption 3.1, given  $\Pi_k^{0,E}$  be the local  $L^2$ -orthogonal projection into  $\mathbb{P}_k(E)$  and  $\Pi_k^{\nabla,E}$   $H^1(E)$ -orthogonal projection defined by (10), then,  $\exists C > 0$ , that depends only on  $\mathcal{K}$  and on the degree  $k$ , such that  $\forall \phi \in H^s(E)$

$$\left| \phi - \Pi_k^{0,E} \phi \right|_{m,E} \leq C h_E^{s-m} |\phi|_{s,E}, \text{ with } m \leq s \leq k + 1, \tag{48}$$

and if  $s \geq 1$

$$\left| \phi - \Pi_k^{\nabla,E} \phi \right|_{m,E} \leq C h_E^{s-m} |\phi|_{s,E}, \text{ with } m \leq s \leq k + 1, \tag{49}$$

where  $|\cdot|_{s,E}$  denotes the  $H^s(E)$ -seminorm.

**Remark 6.** The results of the previous lemma can be easily extended to the vector case of  $\phi \in [H^s(E)]^d$ , with  $d \in \mathbb{N}$ , where the projection operators are defined component-wise  $\Pi_k^{0,E} : [L^2(E)]^d \rightarrow [\mathbb{P}_k(E)]^d$  and  $\Pi_k^{\nabla,E} : [H^1(E)]^d \rightarrow [\mathbb{P}_k(E)]^d$ .

**Lemma 5.** Under Assumption 3.1, let  $u \in H^s(\Omega)$ ,  $1 \leq s \leq k + 1$ , there exists  $C > 0$  such that  $\forall h, \exists u_1 \in \mathcal{V}_{h,k}$  satisfying

$$\|u - u_1\|_{L^2(\Omega)} + h \|\nabla u - \nabla u_1\|_{L^2(\Omega)} \leq C h^s |u|_{s,\Omega}, \tag{50}$$

where  $C$  is a positive constant, depending only on  $k$  and on the mesh regularity (the aspect ratio of  $\mathcal{M}_h$ ).

**Theorem 5.** Let  $u \in H^s(\Omega) \cap H_0^1(\Omega)$  and  $f \in H^{\max\{0, s-2\}}(\Omega)$ , with  $1 \leq s \leq k+1$ , be the solution and the right-hand side of (1), respectively. Then,  $\exists C_{EN} > 0$  independent of  $h$  such that the unique solution  $u_h \in \mathcal{V}_{h,k}$  of problem (25) satisfies the following error estimate:

$$\|u - u_h\|_{\Omega} \leq C_{EN} h^{s-1} (|u|_{s,\Omega} + |f|_{\max\{0, s-2\}, \Omega}). \tag{51}$$

**Proof.** Let  $u_1$  be given by Lemma 5. Applying the triangle inequality, we have

$$\|u - u_h\|_{\Omega} \leq \|u - u_1\|_{\Omega} + \|u_1 - u_h\|_{\Omega}. \tag{52}$$

We deal with the two terms separately. The first can be bounded applying (50) and the regularity hypothesis on  $\mathcal{K}$  (20) and  $\gamma$ , i.e.

$$\begin{aligned} \|u - u_1\|_{\Omega}^2 &= \sum_{E \in \mathcal{M}_h} \left\| \sqrt{\mathcal{K}} \nabla (u - u_1) \right\|_{L^2(E)}^2 + \left\| \sqrt{\gamma} \Pi_k^{0,E} (u - u_1) \right\|_{L^2(E)}^2 \\ &\leq \sum_{E \in \mathcal{M}_h} \mathcal{K}_E^\wedge \|\nabla u - \nabla u_1\|_{L^2(E)}^2 + \|\gamma\|_{L^\infty(E)} \|u - u_1\|_{L^2(E)}^2 \\ &\lesssim \max \left\{ \left( \max_E \mathcal{K}_E^\wedge \right), \left( \max_E \|\gamma\|_{L^\infty(E)} \right) h^2 \right\} h^{2(s-1)} |u|_{s,\Omega}^2, \end{aligned} \tag{53}$$

where  $\lesssim$  denotes that there exists a constant independent of  $h$  and of the problem's parameters. This notation is widely used in the following.

On the other hand, in order to deal with the second term of (52) let  $\varepsilon_h = u_1 - u_h$ . First, applying the coercivity of the bilinear form  $B_h$  (44), problems (25) and (8)

$$\begin{aligned} \Xi_* \|\varepsilon_h\|_{\Omega}^2 &\leq B_h(\varepsilon_h, \varepsilon_h) = \sum_{E \in \mathcal{M}_h} B_h^E(u_1 - u, \varepsilon_h) + B_h^E(u, \varepsilon_h) - (f, \Pi_k^{0,E} \varepsilon_h)_E \\ &= \sum_{E \in \mathcal{M}_h} B_h^E(u_1 - u, \varepsilon_h) + B_h^E(u, \varepsilon_h) - B^E(u, \varepsilon_h) + (f, \varepsilon_h - \Pi_k^{0,E} \varepsilon_h)_E \end{aligned} \tag{54}$$

The first term is estimated using the continuity of  $B$  (40) and (53):

$$\begin{aligned} B(u_1 - u, \varepsilon_h) &\leq \Xi^* \|u - u_1\|_{\Omega} \|\varepsilon_h\|_{\Omega} \\ &\lesssim \Xi^* \sqrt{\max \left\{ \left( \max_E \mathcal{K}_E^\wedge \right), \left( \max_E \|\gamma\|_{L^\infty(E)} \right) h^2 \right\}} h^{s-1} |u|_{s,\Omega} \|\varepsilon_h\|_{\Omega} \end{aligned} \tag{55}$$

Regarding the second and third local terms, they provide the approximation error with respect to polynomials. Applying definitions of  $B_h^E$  and  $B$ , we can split them as

$$B_h^E(u, \varepsilon_h) - B^E(u, \varepsilon_h) = a_h^E(u, \varepsilon_h) - a^E(u, \varepsilon_h) + b_h^E(u, \varepsilon_h) - b^E(u, \varepsilon_h) + c_h^E(u, \varepsilon_h) - c^E(u, \varepsilon_h). \tag{56}$$

The first and the second term of (56) can be bounded exploiting [2, Lemma 5.3] and, since  $[\mathbb{P}_{k-1}(E)]^2 \subset \mathcal{P}_{k,\ell_E} \forall \ell_E \geq 0$ , we can apply (48), i.e. for each  $v \in H^r(E)$

$$\|\nabla v - \Pi_p^{0,E} \nabla v\|_{L^2(E)} \leq \|\nabla v - \Pi_{k-1}^{0,E} \nabla v\|_{L^2(E)} \lesssim h_E^{r-1} |v|_{r,E}, \tag{57}$$

and we obtain

$$\begin{aligned} a_h^E(u, \varepsilon_h) - a^E(u, \varepsilon_h) &= \left( \mathcal{K} \Pi_p^{0,E} \nabla u, \Pi_p^{0,E} \nabla \varepsilon_h \right)_E - \left( \mathcal{K} \nabla u, \nabla \varepsilon_h \right)_E \\ &\leq \left\| \Pi_p^{0,E} (\mathcal{K} \nabla u) - \mathcal{K} \nabla u \right\|_{L^2(E)} \left\| \nabla \varepsilon_h - \Pi_p^{0,E} \nabla \varepsilon_h \right\|_{L^2(E)} \\ &\quad + \left\| \Pi_p^{0,E} \nabla u - \nabla u \right\|_{L^2(E)} \left\| \mathcal{K} \nabla \varepsilon_h - \Pi_p^{0,E} (\mathcal{K} \nabla \varepsilon_h) \right\|_{L^2(E)} \\ &\quad + \mathcal{K}_E^\wedge \left\| \Pi_p^{0,E} \nabla u - \nabla u \right\|_{L^2(E)} \left\| \nabla \varepsilon_h - \Pi_p^{0,E} \nabla \varepsilon_h \right\|_{L^2(E)} \\ &\lesssim h_E^{s-1} |\mathcal{K} \nabla u|_{s-1,E} \|\nabla \varepsilon_h\|_{L^2(E)} + h_E^{s-1} |u|_{s,E} \|\mathcal{K} \nabla \varepsilon_h\|_{L^2(E)} + \mathcal{K}_E^\wedge h_E^{s-1} |u|_{s,E} \|\nabla \varepsilon_h\|_{L^2(E)} \\ &\lesssim \frac{\|\mathcal{K}\|_{W^{s-1,\infty}(E)}}{\sqrt{\mathcal{K}_E^\vee}} h_E^{s-1} |u|_{s,E} \left\| \sqrt{\mathcal{K}} \nabla \varepsilon_h \right\|_{L^2(E)}. \end{aligned} \tag{58}$$

The third and the fourth term of (56) can be bounded applying the estimate in [2, Lemma 5.3] and the polynomial approximation estimate (48), i.e.

$$\begin{aligned} b_h^E(u, \varepsilon_h) - b^E(u, \varepsilon_h) &= \left( \beta \cdot \Pi_{k-1}^{0,E} \nabla u, \Pi_k^{0,E} \varepsilon_h \right)_E - \left( \beta \cdot \nabla u, \varepsilon_h \right)_E \\ &\leq \left\| \Pi_{k-1}^{0,E} (\beta \cdot \nabla u) - \beta \cdot \nabla u \right\|_{L^2(E)} \left\| \varepsilon_h - \Pi_k^{0,E} \varepsilon_h \right\|_{L^2(E)} \\ &\quad + \left\| \Pi_{k-1}^{0,E} \nabla u - \nabla u \right\|_{L^2(E)} \left\| \beta \varepsilon_h - \Pi_{k-1}^{0,E} (\beta \varepsilon_h) \right\|_{L^2(E)} \\ &\quad + \|\beta\|_{L^\infty(E)} \left\| \Pi_{k-1}^{0,E} \nabla u - \nabla u \right\|_{L^2(E)} \left\| \varepsilon_h - \Pi_k^{0,E} \varepsilon_h \right\|_{L^2(E)} \end{aligned}$$

$$\begin{aligned} &\lesssim h_E^s |\beta \nabla u|_{s-1,E} \|\nabla \varepsilon_h\|_{L^2(E)} + h_E^s |u|_{s,E} |\beta \varepsilon_h|_{1,E} + \|\beta\|_{L^\infty(E)} h_E^s |u|_{s,E} \|\nabla \varepsilon_h\|_{L^2(E)} \\ &\lesssim \|\beta\|_{W^{s-1,\infty}(E)} h_E^s |u|_{s,E} \|\nabla \varepsilon_h\|_{L^2(E)}. \end{aligned} \tag{59}$$

The last two terms of (56) can be bounded applying the estimate in [2, Lemma 5.3] and the polynomial approximation estimate (48), i.e.

$$\begin{aligned} c_h^E(u, \varepsilon_h) - c^E(u, \varepsilon_h) &= (\gamma \Pi_k^{0,E} u, \Pi_k^{0,E} \varepsilon_h)_E - (\gamma u, \varepsilon_h)_E \\ &\leq \|\Pi_k^{0,E}(\gamma u) - \gamma u\|_{L^2(E)} \|\varepsilon_h - \Pi_k^{0,E} \varepsilon_h\|_{L^2(E)} \\ &\quad + \|\Pi_k^{0,E} u - u\|_{L^2(E)} \|\gamma \varepsilon_h - \Pi_k^{0,E}(\gamma \varepsilon_h)\|_{L^2(E)} \\ &\quad + \|\gamma\|_{L^\infty(E)} \|\Pi_k^{0,E} u - u\|_{L^2(E)} \|\varepsilon_h - \Pi_k^{0,E} \varepsilon_h\|_{L^2(E)} \\ &\lesssim h_E^{s+1} |\gamma u|_{s,E} \|\nabla \varepsilon_h\|_{L^2(E)} + h_E^{s+1} |u|_{s,E} |\gamma \varepsilon_h|_{1,E} + \|\gamma\|_{L^\infty(E)} h_E^{s+1} |u|_{s,E} \|\nabla \varepsilon_h\|_{L^2(E)} \\ &\lesssim h_E^{s+1} \|\gamma\|_{W^{s,\infty}(E)} |u|_{s,E} \|\nabla \varepsilon_h\|_{L^2(E)} \end{aligned} \tag{60}$$

The last term of (54) can be bounded applying the definition of  $\Pi_0^{0,E}$ , the Cauchy–Schwarz inequality and the approximation property (48), i.e.

$$\begin{aligned} \sum_{E \in \mathcal{M}_h} (f, \varepsilon_h - \Pi_k^{0,E} \varepsilon_h)_E &= \sum_{E \in \mathcal{M}_h} (f - \Pi_k^{0,E} f, \varepsilon_h - \Pi_k^{0,E} \varepsilon_h)_E \\ &\leq \sum_{E \in \mathcal{M}_h} \|f - \Pi_k^{0,E} f\|_{L^2(E)} \|\varepsilon_h - \Pi_k^{0,E} \varepsilon_h\|_{L^2(E)} \\ &\lesssim h^{s-1} |f|_{\max\{0, s-2\}, \Omega} \sum_{E \in \mathcal{M}_h} \frac{1}{\sqrt{\mathcal{K}_E^V}} \|\sqrt{\mathcal{K}} \nabla \varepsilon_h\|_{L^2(E)} \\ &\lesssim \frac{1}{\min_E \sqrt{\mathcal{K}_E^V}} h^{s-1} |f|_{\max\{0, s-2\}, \Omega} \|\varepsilon_h\|_\Omega. \end{aligned} \tag{61}$$

Finally, considering together (55), (58), (59), (60) and (61), and substituting them into (54), we obtain

$$\begin{aligned} \Xi_* \|\varepsilon_h\|_\Omega^2 &\lesssim \Xi_* \sqrt{\max\left\{ \left(\max_E \mathcal{K}_E^\wedge\right), \left(\max_E \|\gamma\|_{L^\infty(E)}\right) h^2 \right\}} h^{s-1} |u|_{s,\Omega} \|\varepsilon_h\|_\Omega \\ &\quad + \sum_{E \in \mathcal{M}_h} \left( \frac{\|\mathcal{K}\|_{W^{s-1,\infty}(E)}}{\sqrt{\mathcal{K}_E^V}} \|\sqrt{\mathcal{K}} \nabla \varepsilon_h\|_{L^2(E)} + h_E^2 \|\gamma\|_{W^{s,\infty}(E)} \|\nabla \varepsilon_h\|_{L^2(E)} \right. \\ &\quad \left. + \|\beta\|_{W^{s-1,\infty}(E)} h_E \|\nabla \varepsilon_h\|_{L^2(E)} \right) h^{s-1} |u|_{s,\Omega} + \frac{1}{\min_E \sqrt{\mathcal{K}_E^V}} h^{s-1} |f|_{\max\{0, s-2\}, \Omega} \|\varepsilon_h\|_\Omega \\ &\lesssim \Xi_* \sqrt{\max\left\{ \left(\max_E \mathcal{K}_E^\wedge\right), \left(\max_E \|\gamma\|_{L^\infty(E)}\right) h^2 \right\}} h^{s-1} |u|_{s,\Omega} \|\varepsilon_h\|_\Omega \\ &\quad + \frac{1}{\min_E \sqrt{\mathcal{K}_E^V}} \max\left\{ \|\mathcal{K}\|_{W^{s-1,\infty}(\Omega)}, h^2 \|\gamma\|_{W^{s,\infty}(\Omega)}, h \|\beta\|_{W^{s-1,\infty}(\Omega)} \right\} h^{s-1} |u|_{s,\Omega} \|\varepsilon_h\|_\Omega \\ &\quad + \frac{1}{\min_E \sqrt{\mathcal{K}_E^V}} h^{s-1} |f|_{\max\{0, s-2\}, \Omega} \|\varepsilon_h\|_\Omega \end{aligned} \tag{62}$$

Considering this last estimate together with (53), we have the thesis (51).  $\square$

**Theorem 6** (*L<sup>2</sup> Error Estimate*). *Let  $\Omega$  be convex. Let  $u \in H^s(\Omega) \cap H_0^1(\Omega)$  and  $f \in H^{\max\{0, s-2\}}(\Omega)$ , with  $1 \leq s \leq k + 1$ , be the solution and the right-hand side of (1), respectively. Then,  $\exists C > 0$  such that the unique solution  $u \in \mathcal{V}_{h,k}$  of problem (25) satisfies the following error estimate:*

$$\|u - u_h\|_{L^2(\Omega)} \leq Ch^s (|u|_{s,\Omega} + |f|_{\max\{0, s-2\}, \Omega}). \tag{63}$$

**Proof.** Let us define the auxiliary problem: let  $\psi \in H^2(\Omega) \cap H_0^1(\Omega)$  the solution of the adjoint problem  $B^*(\psi, v) = (u - u_h, v)_\Omega \forall v \in H_0^1(\Omega)$ , where, given  $a$  and  $c$  as in (4) and (6),

$$B^*(\psi, v) := a(\psi, v) - \int_\Omega (\beta \cdot \nabla \psi) v + c(\psi, v). \tag{64}$$

By definition,  $\mathcal{B}(u, v) = B^*(v, u)$  for each  $u, v \in H_0^1(\Omega)$  and we get:

$$|\psi|_2 \lesssim \|u - u_h\|_{L^2(\Omega)}, \quad \|\nabla \psi\|_{L^2(\Omega)} \lesssim \|u - u_h\|_{L^2(\Omega)}, \tag{65}$$

where, as previously,  $\lesssim$  denotes that there exists a constant independent of  $h$  and of the problem's parameters. Let  $\psi_I$  denote the interpolant of  $\psi$  for which it holds true

$$\|\psi - \psi_I\|_{L^2(\Omega)} + h \|\nabla\psi - \nabla\psi_I\|_{L^2(\Omega)} \leq Ch^2 |\psi|_{2,\Omega} . \tag{66}$$

Applying the auxiliary problem, the discrete problem (25) and the definition of  $\mathcal{B}$  (3), we have

$$\begin{aligned} \|u - u_h\|_{L^2(\Omega)}^2 &= \mathcal{B}^*(\psi, u - u_h) = \mathcal{B}(u - u_h, \psi) = \mathcal{B}(u, \psi - \psi_I) + \mathcal{B}(u, \psi_I) - \mathcal{B}(u_h, \psi) \\ &= \mathcal{B}(u, \psi - \psi_I) + (f, \psi_I)_\Omega - \mathcal{B}(u_h, \psi) \\ &= \mathcal{B}(u, \psi - \psi_I) + (f, \psi_I)_\Omega - \sum_{E \in \mathcal{M}_h} \left( f, \Pi_k^{0,E} \psi_I \right)_E + \mathcal{B}_h(u_h, \psi_I) - \mathcal{B}(u_h, \psi) \\ &= \mathcal{B}(u - u_h, \psi - \psi_I) + \sum_{E \in \mathcal{M}_h} \left( f, \psi_I - \Pi_k^{0,E} \psi_I \right)_E + \mathcal{B}_h(u_h, \psi_I) - \mathcal{B}(u_h, \psi_I) . \end{aligned} \tag{67}$$

Let us consider the terms of the previous relation separately. First, applying the continuity of  $\mathcal{B}$  (40), proceeding as (53), and using (65) and (66), we have, for the first term,

$$\begin{aligned} \mathcal{B}(u - u_h, \psi - \psi_I) &\leq \Xi^* \|u - u_h\|_\Omega \|\psi - \psi_I\|_\Omega \\ &\lesssim \Xi^* \sqrt{\max \left\{ \left( \max_E \mathcal{K}_E^\wedge \right), \left( \max_E \|\gamma\|_{L^\infty(E)} \right) h^2 \right\}} h \|u - u_h\|_\Omega |\psi|_{2,\Omega} \\ &\lesssim \Xi^* \sqrt{\max \left\{ \left( \max_E \mathcal{K}_E^\wedge \right), \left( \max_E \|\gamma\|_{L^\infty(E)} \right) h^2 \right\}} h \|u - u_h\|_\Omega \|u - u_h\|_{L^2(\Omega)} . \end{aligned} \tag{68}$$

The second term of (67) is estimated using the orthogonality property of  $\Pi_0^{0,E}$ , we have that  $\forall E \in \mathcal{M}_h$

$$\|\psi_I - \Pi_k^{0,E} \psi_I\|_{L^2(E)} \leq \|\psi_I - \Pi_k^{0,E} \psi\|_{L^2(E)} , \tag{69}$$

hence we have

$$\begin{aligned} \sum_{E \in \mathcal{M}_h} \left( f, \psi_I - \Pi_k^{0,E} \psi_I \right)_E &= \sum_{E \in \mathcal{M}_h} \left( f - \Pi_k^{0,E} f, \psi_I - \Pi_k^{0,E} \psi_I \right)_E \\ &\leq \sum_{E \in \mathcal{M}_h} \|f - \Pi_k^{0,E} f\|_{L^2(E)} \|\psi_I - \Pi_k^{0,E} \psi_I\|_{L^2(E)} \\ &\lesssim h^s |f|_{\max\{0, s-2\}, \Omega} |\psi|_{2,\Omega} \lesssim h^s |f|_{\max\{0, s-2\}, \Omega} \|u - u_h\|_{L^2(\Omega)} . \end{aligned} \tag{70}$$

where (50), (48) and (65) are applied, omitting higher order terms.

Finally, considering (67) we have to bound  $\mathcal{B}_h(u_h, \psi_I) - \mathcal{B}(u_h, \psi_I)$ . Applying definitions of  $\mathcal{B}_h$  and  $\mathcal{B}$ , we can split them as

$$\begin{aligned} \mathcal{B}_h(u_h, \psi_I) - \mathcal{B}(u_h, \psi_I) &= \sum_{E \in \mathcal{M}_h} a_h^E(u_h, \psi_I) - a^E(u_h, \psi_I) \\ &+ b_h^E(u_h, \psi_I) - b^E(u_h, \psi_I) + c_h^E(u_h, \psi_I) - c^E(u_h, \psi_I) . \end{aligned} \tag{71}$$

Considering for each  $E \in \mathcal{M}_h$  the local contribution, we can apply [2, Lemma 5.3], orthogonality properties similar to (69), adding and subtracting terms, the polynomial approximation property (48), the estimates (66) and (65) for  $\psi$ , hence we obtain the following local estimates

$$\begin{aligned} a_h^E(u_h, \psi_I) - a^E(u_h, \psi_I) &= \left( \mathcal{K} \Pi_p^{0,E} \nabla u_h, \Pi_p^{0,E} \nabla \psi_I \right)_E - \left( \mathcal{K} \nabla u_h, \nabla \psi_I \right)_E \\ &\leq \left\| \Pi_p^{0,E} (\mathcal{K} \nabla u_h) - \mathcal{K} \nabla u_h \right\|_{L^2(E)} \left\| \nabla \psi_I - \Pi_p^{0,E} \nabla \psi \right\|_{L^2(E)} \\ &+ \left\| \Pi_p^{0,E} \nabla u_h - \nabla u_h \right\|_{L^2(E)} \left( \left\| \mathcal{K} \nabla \psi_I - \Pi_p^{0,E} (\mathcal{K} \nabla \psi) \right\|_{L^2(E)} + \mathcal{K}_E^\wedge \left\| \nabla \psi_I - \Pi_p^{0,E} \nabla \psi \right\|_{L^2(E)} \right) \\ &\lesssim \left( \left\| \Pi_p^{0,E} (\mathcal{K} \nabla u) - \mathcal{K} \nabla u \right\|_{L^2(E)} + \left\| \mathcal{K} \nabla u - \mathcal{K} \nabla u_h \right\|_{L^2(E)} \right) \\ &\cdot \left( \left\| \nabla \psi_I - \nabla \psi \right\|_{L^2(E)} + \left\| \nabla \psi - \Pi_p^{0,E} \nabla \psi \right\|_{L^2(E)} \right) \\ &+ \left( \left\| \Pi_p^{0,E} \nabla u - \nabla u \right\|_{L^2(E)} + \left\| \nabla u - \nabla u_h \right\|_{L^2(E)} \right) \\ &\cdot \left( \left\| \mathcal{K} \nabla \psi_I - \mathcal{K} \nabla \psi \right\|_{L^2(E)} + \left\| \mathcal{K} \nabla \psi - \Pi_p^{0,E} (\mathcal{K} \nabla \psi) \right\|_{L^2(E)} \right) \\ &+ \mathcal{K}_E^\wedge \left( \left\| \nabla \psi_I - \nabla \psi \right\|_{L^2(E)} + \left\| \nabla \psi - \Pi_p^{0,E} \nabla \psi \right\|_{L^2(E)} \right) \\ &\lesssim \left( h_E^{s-1} |u|_{s,E} + \max \left\{ \frac{\sqrt{\mathcal{K}_E^\wedge}}{\|\mathcal{K}\|_{W^{s-1,\infty}(E)}}, \frac{1}{\sqrt{\mathcal{K}_E^\vee}} \right\} \|u - u_h\|_E \right) \|\mathcal{K}\|_{W^{s-1,\infty}(E)} h |\psi|_{2,\Omega} \end{aligned}$$

$$\lesssim \left( h_E^{s-1} |u|_{s,E} + \max \left\{ \frac{\sqrt{\mathcal{K}_E^\wedge}}{\|\mathcal{K}\|_{W^{s-1,\infty}(E)}}, \frac{1}{\sqrt{\mathcal{K}_E^\vee}} \right\} \|u - u_h\|_E \right) \|\mathcal{K}\|_{W^{s-1,\infty}(E)} h \|u - u_h\|_{L^2(\Omega)}$$

and, similarly,

$$\begin{aligned} b_h^E(u_h, \psi_I) - b^E(u_h, \psi_I) &= (\beta \cdot \Pi_{k-1}^{0,E} \nabla u_h, \Pi_k^{0,E} \psi_I)_E - (\beta \cdot \nabla u_h, \psi_I)_E \\ &\lesssim \left( h_E^{s-1} |u|_{s,E} + \frac{1}{\sqrt{\mathcal{K}_E^\vee}} \|u - u_h\|_E \right) \|\beta\|_{W^{s-1,\infty}(E)} h^{\min\{2,k\}} \|u - u_h\|_{L^2(\Omega)} \end{aligned}$$

and

$$\begin{aligned} c_h^E(u_h, \psi_I) - c^E(u_h, \psi_I) &= (\gamma \Pi_k^{0,E} u_h, \Pi_k^{0,E} \psi_I)_E - (\gamma u_h, \psi_I)_E \\ &\lesssim (h_E^s |u|_{s,E} + \|u - u_h\|_{L^2(E)}) \|\gamma\|_{W^{s,\infty}(E)} h^2 \|u - u_h\|_{L^2(\Omega)}. \end{aligned}$$

Hence, the estimate (71) results

$$\begin{aligned} &B_h(u_h, \psi_I) - B(u_h, \psi_I) \\ &\lesssim \max_{E \in \mathcal{M}_h} \left( \max \left\{ \|\mathcal{K}\|_{W^{s-1,\infty}(E)}, \|\beta\|_{W^{s-1,\infty}(E)} h^{\min\{1,k-1\}}, \|\gamma\|_{W^{s,\infty}(E)} h^2 \right\} \right) \\ &\cdot h^s |u|_{s,\Omega} \|u - u_h\|_{L^2(\Omega)} \\ &+ \max_{E \in \mathcal{M}_h} \left( \max \left\{ \frac{\sqrt{\mathcal{K}_E^\wedge}}{\|\mathcal{K}\|_{W^{s-1,\infty}(E)}}, \frac{1}{\sqrt{\mathcal{K}_E^\vee}} \right\} \right) \\ &\cdot \max_{E \in \mathcal{M}_h} \left( \max \left\{ \|\mathcal{K}\|_{W^{s-1,\infty}(E)}, \|\beta\|_{W^{s-1,\infty}(E)} h^{\min\{1,k-1\}} \right\} \right) \\ &\cdot C_{EN} h^s (|u|_{s,\Omega} + |f|_{s-1}) \|u - u_h\|_{L^2(\Omega)} \\ &+ C_P \max_E \left( \frac{1}{\sqrt{\mathcal{K}_E^\vee}} \right) C_{EN} h^s (|u|_{s,\Omega} + |f|_{s-1}) h^2 \|\gamma\|_{W^{s,\infty}(\Omega)} \|u - u_h\|_{L^2(\Omega)} \end{aligned} \tag{72}$$

where we apply the error estimate (51) and a Poincaré inequality.

Finally, applying (68), (70), (72) to (67) and simplifying, we obtain the thesis (63).  $\square$

### 6. Computation of $\Pi_p^{0,E} \nabla$

---

**Algorithm 1** Algorithm for the computation of  $\ell_E$  and of the corresponding right-hand side on a given polygon.

---

**Input:** A polygon  $E \in \mathcal{M}_h$

- 1: Let  $\ell_E$  be the smallest number satisfying (76).
  - 2: Compute the matrix  $B$  corresponding to  $\ell_E$  defined by (74).
  - 3: Compute the factor  $R$  of a QR decomposition of  $B$  (Householder QR is advisable).
  - 4:  $N \leftarrow$  number of diagonal elements of  $R$  whose absolute value is  $\geq 1e - 11$ .
  - 5: **while**  $N < kN_E + \frac{k(k-1)}{2} - 1$  **do**
  - 6:  $\ell_E \leftarrow \ell_E + 1$ .
  - 7: Compute  $\tilde{B} = \begin{pmatrix} \tilde{C}_{k+\ell_E}^\partial & 0 \end{pmatrix}$  such that  $\left( \tilde{C}_{k+\ell_E}^\partial \right)_{ij} = \left( \nabla \varphi_j^\partial \cdot \mathbf{t}, \tilde{r}_i \right)_{\partial E}$ ,  $\forall \tilde{r}_i$  basis of homogeneous polynomials of degree  $k + \ell_E$ .
  - 8:  $R \leftarrow [B; R]$
  - 9: Using Givens rotations, update  $R$  to triangular matrix.
  - 10:  $B \leftarrow [B; \tilde{B}]$
  - 11:  $N \leftarrow$  number of diagonal elements of  $R$  whose absolute value is  $\geq 1e - 11$ .
  - 12: **end while**
  - 13: **return**  $\ell_E, B$ .
- 

In this section, we analyze the computation of  $\Pi_p^{0,E} \nabla$  and, following [17], we propose an algorithm that provides the polynomial projection degree ensuring stability. The algorithm is based on an incremental QR decomposition of the right-hand side of the linear system that needs to be solved to compute the matrix representing the projection operator. In particular, let  $E \in \mathcal{M}_h$  be given and let  $\{\varphi_j\}_{j=1}^{\dim \mathcal{V}_{h,k}^E}$  be a lagrangian basis of  $\mathcal{V}_{h,k}^E$  with respect to the degrees of freedom. In particular, let  $\{\varphi_j^\partial\}_{j=1}^{kN_E}$  and  $\{\varphi_j^\circ\}_{j=1}^{\dim \mathbb{P}_{k-2}(E)}$  be the

subsets of basis functions lagrangian with respect to the boundary and the internal degrees of freedom, respectively. Furthermore, given any value of  $\ell_E$ , let  $\mathbf{M} = \{m_i\}_{i=1}^{\dim[\mathbb{P}_{k-1}(E)]^2}$  be a scaled monomial basis of  $[\mathbb{P}_{k-1}(E)]^2$  and let  $\mathbf{C} = \{\text{curl } r_i\}_{i=1}^{\dim \mathbb{P}_{k+\ell_E}(E) - \dim \mathbb{P}_k(E)}$  be a basis of  $\text{curl} \left( \mathbb{P}_{k+\ell_E}(E) \setminus \mathbb{P}_k(E) \right)$ . Let  $B$  be the matrix with the following block structure

$$B = \begin{pmatrix} E_{k-1}^\partial & E_{k-1}^\circ \\ C_{k,\ell_E}^\partial & 0 \end{pmatrix}, \tag{73}$$

where

$$\begin{aligned} (E_{k-1}^\partial)_{i,j} &= \left( \nabla \varphi_j^\partial, m_i \right)_E, & \forall i = 1, \dots, \dim [\mathbb{P}_{k-1}(E)]^2, j = 1, \dots, kN_E \\ (E_{k-1}^\circ)_{i,j} &= \left( \nabla \varphi_j^\circ, m_i \right)_E, & \forall i = 1, \dots, \dim [\mathbb{P}_{k-1}(E)]^2, j = 1, \dots, \dim \mathbb{P}_{k-2}(E) \\ (C_{k,\ell_E}^\partial)_{i,j} &= \left( \nabla \varphi_j^\partial, t, r_i \right)_{\partial E}, & \forall i = 1, \dots, \dim \mathbb{P}_{k+\ell_E}(E) - \dim \mathbb{P}_k(E), j = 1, \dots, kN_E \end{aligned} \tag{74}$$

We notice that the matrices  $E_{k-1}^\partial$  and  $E_{k-1}^\circ$  are used in the computation of the standard projector of the stabilized VEM method and that our approach requires the additional computation of the matrix  $C_{k,\ell_E}^\partial$ , that involves only 1D boundary integrals. Hence, the matrix  $\hat{\Pi}$  representing the projection defined in (14) is the solution of the matrix equation

$$G\hat{\Pi} = B, \tag{75}$$

where  $G$  is the mass matrix of the polynomial basis  $\mathbf{M} \cup \mathbf{C}$ . In order to get a stable scheme, we need to ensure that the rank of  $\hat{\Pi}$  is at least  $kN_E + \frac{k(k-1)}{2} - 1$ , and since  $G$  is symmetric and positive definite, this is guaranteed if the rank of  $B$  is  $kN_E + \frac{k(k-1)}{2} - 1$ . Following [17], we employ an incremental Q-less QR decomposition of  $B$ , with increasing polynomial degrees, which is described in Algorithm 1. First, we set  $\ell_E$  to be the smallest integer satisfying

$$\dim \mathcal{P}_{k,\ell_E} \geq \dim \nabla \mathcal{V}_{h,k}^E \iff (\ell_E + k + 1)(\ell_E + k + 2) \geq 2kN_E, \tag{76}$$

which is a necessary condition for the injectivity of  $\Pi_P^{0,E} \nabla$ . We then compute the  $B$  matrix corresponding to  $\ell_E$  and the factor  $R$  of an Householder QR-decomposition of  $B$ . The rank of  $B$  is then computed as the number of diagonal elements of  $R$  that are greater than a chosen threshold (that we chose equal to  $\epsilon - 11$ ). If the rank is not large enough, we compute additional rows of the right-hand side corresponding to homogeneous polynomials of degree  $\ell_E + 1$  and we update the  $R$  matrix by using Givens rotations on the additional rows, until we reach the desired rank. Notice that the computational cost of the algorithm is equivalent to the one of computing the  $R$  matrix of a QR decomposition of the final right-hand side. Applying Algorithm 1, we identify the minimum  $\ell_E$  providing numerically the coercivity and the corresponding right-hand side  $B$ . Then, we compute the matrix  $G$  and solve (75).

**Remark 7.** Notice that considering the second decomposition of  $\mathcal{P}_{k,\ell_E}$  in (13) together with Lemma 2, we can rewrite Algorithm 1 computing the incremental QR decomposition only for the basis functions  $\{\varphi_j^\partial\}_{j=1}^{kN_E}$  related to the boundary degrees of freedom.

## 7. Numerical results

In this section, we first carry out a numerical investigation on the stability of the method given by the application of Algorithm 1 on different sets of polygons, then we present some convergence tests. In all the numerical tests we use the following definition of the scalar monomial basis of  $\mathbb{P}_k(E)$ :

$$m_i := \left( 2 \frac{\mathbf{x} - \mathbf{x}_E}{h_E} \right)^{\alpha_i}, \quad i = 1, \dots, n_k.$$

In particular, the factor 2 allows for a dramatic reduction of the ill-conditioning of the matrix, as shown in [32]. These monomials are also used in the definition of internal degrees of freedom.

### 7.1. Coercivity tests

We here take into consideration elements with different polygonal shape and we apply Algorithm 1 to get a stable local discrete bilinear form. Then, we build the corresponding local stiffness matrix  $A_h^E$  related to the local discrete bilinear form  $a_h^E$ . In all the tests, we report the square root of the smallest non-vanishing singular value  $\sigma_E$  to estimate the square root of the coercivity constant in Theorem 1. For each set of polygons, we perform this test for  $k = 2, 3, 4$ . Analogous tests for  $k = 1$  are performed in [17], where a lowest-order version of the scheme is introduced.

#### 7.1.1. Regular polygons

We first consider the test case of regular polygons whose vertices are given by the set  $\left\{ \cos \left( \frac{2\pi(i-1)}{N_E} \right), \sin \left( \frac{2\pi(i-1)}{N_E} \right) \right\}_{i=1}^{N_E}$ . The results for the cases  $k = 2, 3, 4$  are reported in Tables 1, 2, 3, respectively.

#### 7.1.2. Concave polygons

Now, we consider the set of concave polygons depicted in Fig. 1. The results for the cases  $k = 2, 3, 4$  are reported in Tables 4, 5, 6, respectively.

**Table 1**

Regular polygons,  $k = 2$ . Values of  $\ell_E$  given by Algorithm 1, in parentheses the smallest value satisfying the necessary condition (76), and computed value of  $\sigma_E$ .

$N_E$	3	4	5	6	7	8	9	10
$\ell_E$	1 (0)	2 (1)	3 (1)	4 (2)	5 (2)	6 (3)	7(3)	8 (3)
$\sigma_E$	6.5e-01	7.0e-01	6.8e-01	6.5e-01	6.2e-01	5.9e-01	5.6e-01	5.3e-01
$N_E$	11	12	13	14	15	16	17	18
$\ell_E$	9 (4)	10 (4)	11 (4)	12 (4)	13 (5)	14 (5)	15 (5)	16 (5)
$\sigma_E$	5.1e-01	4.9e-01	4.8e-01	4.6e-01	4.5e-01	4.3e-01	4.2e-01	4.1e-01

**Table 2**

Regular polygons,  $k = 3$ . Values of  $\ell_E$  given by Algorithm 1, in parentheses the smallest value satisfying the necessary condition (76), and computed value of  $\sigma_E$ .

$N_E$	3	4	5	6	7	8	9	10
$\ell_E$	0 (0)	1 (1)	2 (1)	3 (2)	4 (2)	5 (3)	6 (3)	7 (4)
$\sigma_E$	4.5e-01	3.9e-01	3.1e-01	2.5e-01	2.8e-01	2.4e-01	2.3e-01	2.0e-01
$N_E$	11	12	13	14	15	16	17	18
$\ell_E$	8 (4)	9 (4)	10 (5)	11 (5)	12 (5)	13 (6)	14 (6)	15 (6)
$\sigma_E$	2.1e-01	1.9e-01	1.9e-01	1.7e-01	1.8e-01	1.7e-01	1.7e-01	1.6e-01

**Table 3**

Regular polygons,  $k = 4$ . Values of  $\ell_E$  given by Algorithm 1, in parentheses the smallest value satisfying the necessary condition (76), and computed value of  $\sigma_E$ .

$N_E$	3	4	5	6	7	8	9	10
$\ell_E$	1 (0)	2 (1)	3 (1)	4 (2)	5 (2)	6 (3)	7 (3)	8 (4)
$\sigma_E$	4.6e-01	4.8e-01	4.2e-01	3.4e-01	2.7e-01	2.3e-01	2.0e-01	1.7e-01
$N_E$	11	12	13	14	15	16	17	18
$\ell_E$	9 (4)	10 (5)	11 (5)	12 (6)	13 (6)	14 (6)	15 (7)	16 (7)
$\sigma_E$	1.5e-01	1.4e-01	1.2e-01	1.1e-01	1.0e-01	9.4e-02	8.8e-02	8.2e-02

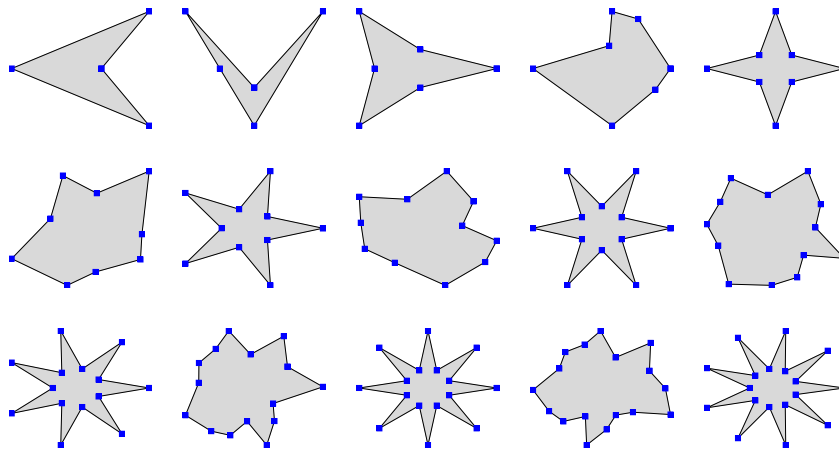


Fig. 1. Concave polygons with  $N_E$  ranging from 4 to 18.

7.1.3. Convex polygons

We here consider the set of convex polygons shown in Fig. 2. In Tables 7, 9, 11, we report the results for  $k = 2, 3, 4$ , respectively. The tables show that in cases of elements with a lot of edges, the value of  $\sigma_E$  might be small. In Tables 8, 10, and 12 we show that, increasing the value of  $\ell_E$  by one, we can enlarge the value of  $\sigma_E$ . In Table 12 we report also the effect of increasing  $\ell_E$  by two, we note an increasing behavior of  $\sigma_E$  w.r.t.  $\ell_E$ .

7.1.4. Hexagon with aligned edges

We consider the set of hexagonal-shape elements with aligned edges depicted in Fig. 3. We perform the test for different order of the method,  $k = 2, 3, 4$ , and we collect the results in Tables 13, 14, 16, respectively.

**Table 4**

Concave polygons,  $k = 2$ . Values of  $\ell_E$  given by Algorithm 1, in parentheses the smallest value satisfying the necessary condition (76), and computed value of  $\sigma_E$ .

$N_E$	4	5	6	7	8	9	10	11
$\ell_E$	1 (1)	1 (1)	3 (2)	2 (2)	4 (3)	3 (3)	5 (3)	4 (4)
$\sigma_E$	3.9e-01	3.5e-02	4.2e-01	1.1e-01	3.9e-01	6.2e-02	3.6e-01	6.4e-02
$N_E$	12	13	14	15	16	17	18	
$\ell_E$	6 (4)	4 (4)	7 (4)	5 (5)	8 (5)	5 (5)	9 (5)	
$\sigma_E$	3.2e-01	2.9e-02	2.5e-01	8.9e-02	1.9e-01	1.4e-02	1.5e-01	

**Table 5**

Concave polygons,  $k = 3$ . Values of  $\ell_E$  given by Algorithm 1, in parentheses the smallest value satisfying the necessary condition (76),  $\sigma_E$ .

$N_E$	4	5	6	7	8	9	10	11
$\ell_E$	1 (1)	2 (1)	3 (2)	3 (2)	5 (3)	3 (3)	6 (4)	4 (4)
$\sigma_E$	2.1e-01	1.8e-01	2.8e-01	1.1e-01	3.1e-01	9.2e-04	2.8e-01	6.3e-03
$N_E$	12	13	14	15	16	17	18	
$\ell_E$	7 (4)	5 (5)	8 (5)	6 (5)	9 (6)	6 (6)	10 (6)	
$\sigma_E$	2.3e-01	1.6e-02	1.6e-01	2.4e-02	1.1e-01	6.3e-03	8.3e-02	

**Table 6**

Concave polygons,  $k = 4$ . Values of  $\ell_E$  given by Algorithm 1, in parentheses the smallest value satisfying the necessary condition (76), and computed value of  $\sigma_E$ .

$N_E$	4	5	6	7	8	9	10	11
$\ell_E$	1 (1)	2 (1)	3 (2)	2 (2)	4 (3)	3 (3)	6 (4)	4 (4)
$\sigma_E$	7.2e-02	5.8e-02	7.1e-02	2.3e-03	6.3e-02	6.1e-04	2.4e-02	5.3e-04
$N_E$	12	13	14	15	16	17	18	
$\ell_E$	8 (5)	5 (5)	9 (6)	6 (6)	10 (6)	7 (7)	11 (7)	
$\sigma_E$	1.8e-01	9.1e-04	1.2e-01	2.9e-03	8.0e-02	2.8e-03	5.4e-02	

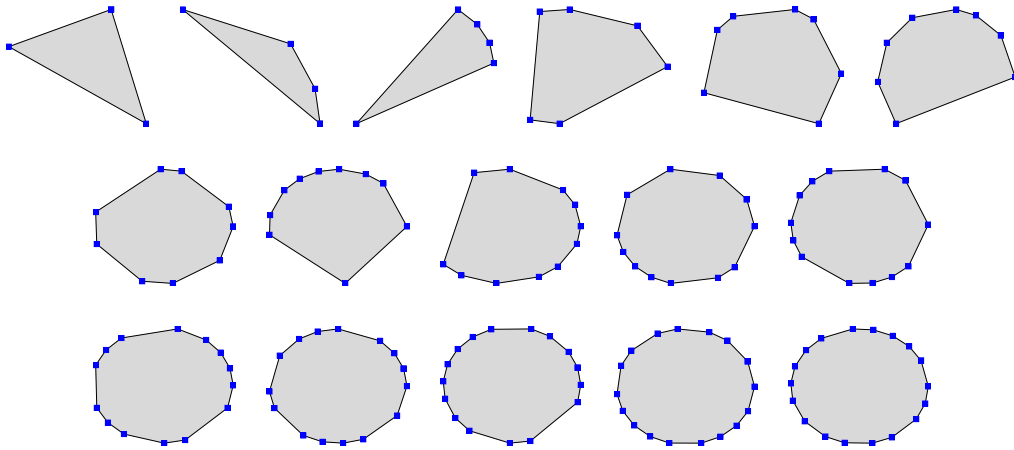


**Fig. 2.** Convex polygons with  $N_E$  ranging from 3 to 18.

**Table 7**

Convex polygons,  $k = 2$ . Values of  $\ell_E$  given by Algorithm 1, in parentheses the smallest value satisfying the necessary condition (76), and computed value of  $\sigma_E$ .

$N_E$	3	4	5	6	7	8	9	10
$\ell_E$	1 (0)	1 (1)	1 (1)	2 (2)	2 (2)	3 (3)	3 (3)	3 (3)
$\sigma_E$	5.0e-01	2.8e-01	1.0e-03	7.9e-02	2.9e-02	2.8e-02	1.3e-02	7.2e-05
$N_E$	11	12	13	14	15	16	17	18
$\ell_E$	4 (4)	4 (4)	4 (4)	4 (4)	5 (5)	5 (5)	5 (5)	5 (5)
$\sigma_E$	5.0e-04	1.0e-04	2.5e-04	2.2e-07	2.8e-04	1.6e-05	9.5e-07	1.9e-08

**Table 8**

Convex polygons,  $k = 2$ . Increased values of  $\ell_E$  with respect to Table 7, in parentheses the smallest value satisfying the necessary condition (76), and computed value of  $\sigma_E$ .

$N_E$	14	14	$N_E$	17	17	$N_E$	18	18
$\ell_E$	4 (4)	5 (4)	$\ell_E$	5 (5)	6 (5)	$\ell_E$	5 (5)	6 (5)
$\sigma_E$	2.2e-07	6.6e-04	$\sigma_E$	9.5e-07	1.6e-04	$\sigma_E$	1.9e-08	9.9e-05

**Table 9**

Convex polygons,  $k = 3$ . Values of  $\ell_E$  given by Algorithm 1, in parentheses the smallest value satisfying the necessary condition (76), and computed value of  $\sigma_E$ .

$N_E$	3	4	5	6	7	8	9	10
$\ell_E$	0 (0)	1 (1)	2 (1)	2 (2)	3 (2)	3 (3)	3 (3)	4 (4)
$\sigma_E$	3.4e-01	4.1e-02	8.3e-03	3.6e-02	3.1e-02	2.2e-03	7.2e-04	5.8e-06
$N_E$	11	12	13	14	15	16	17	18
$\ell_E$	4 (4)	5 (4)	5 (5)	5 (5)	6 (5)	6 (6)	6 (6)	6 (6)
$\sigma_E$	7.9e-05	2.7e-06	7.6e-05	9.7e-07	1.9e-05	3.1e-07	6.1e-08	5.2e-08

**Table 10**

Convex polygons,  $k = 3$ . Increased values of  $\ell_E$  with respect to Table 9, in parentheses the smallest value satisfying the necessary condition (76), and computed value of  $\sigma_E$ .

$N_E$	14	14	$N_E$	16	16
$\ell_E$	5 (5)	6 (5)	$\ell_E$	6 (6)	7 (6)
$\sigma_E$	9.7e-07	2.3e-04	$\sigma_E$	3.1e-07	8.9e-06
$N_E$	17	17	$N_E$	18	18
$\ell_E$	6 (6)	7 (6)	$\ell_E$	6 (6)	7 (6)
$\sigma_E$	6.1e-08	2.3e-06	$\sigma_E$	5.2e-08	5.5e-07
					1.3e-05

**Table 11**

Convex polygons,  $k = 4$ . Values of  $\ell_E$  given by Algorithm 1, in parentheses the smallest value satisfying the necessary condition (76), and computed value of  $\sigma_E$ .

$N_E$	3	4	5	6	7	8	9	10
$\ell_E$	1 (0)	1 (1)	1 (1)	2 (2)	2 (2)	3 (3)	3 (3)	4 (4)
$\sigma_E$	3.5e-01	2.9e-02	2.2e-06	1.6e-02	1.6e-05	1.1e-04	3.6e-05	7.4e-07
$N_E$	11	12	13	14	15	16	17	18
$\ell_E$	4 (4)	5 (5)	5 (5)	6 (6)	6 (6)	6 (6)	7 (7)	7 (7)
$\sigma_E$	1.9e-06	2.6e-06	1.5e-06	2.7e-06	1.6e-06	7.9e-08	2.4e-07	1.1e-07

**Table 12**

Convex polygons,  $k = 4$ . Increased values of  $\ell_E$  with respect to Table 11, in parentheses the smallest value satisfying the necessary condition (76), and computed value of  $\sigma_E$ .

$N_E$	10	10	$N_E$	16	16	16
$\ell_E$	4 (4)	5 (4)	$\ell_E$	6 (6)	7 (6)	8 (6)
$\sigma_E$	7.4e-07	1.8e-05	$\sigma_E$	7.9e-08	2.6e-07	7.6e-06
$N_E$	17	17	$N_E$	18	18	18
$\ell_E$	7 (7)	8 (7)	$\ell_E$	7 (7)	8 (7)	9 (7)
$\sigma_E$	2.4e-07	2.8e-06	$\sigma_E$	1.1e-07	4.9e-07	1.5e-05

As in previous cases, Tables 14 and 16 show that in the cases of elements with a lot of edges, the computed  $\sigma_E$  might be small. In these cases, increasing the value of  $\ell_E$  we obtain larger  $\sigma_E$ , as depicted in . In particular, for  $k = 4$  we provide Table 17 with the values of  $\ell_E$  such that the values of  $\sigma_E$  are larger than  $1e-06$ .

7.1.5. Triangle with aligned edges

Finally, we take into consideration the case of the triangles with aligned edges shown in Fig. 4. The singular values  $\sigma_E$  and the computed  $\ell_E$  are shown in Tables 18, 19, 20 for the cases  $k = 2, 3, 4$ , respectively.

7.2. Convergence tests

In this section, we perform three tests solving problem (1) on the unit square, tessellated by three families of meshes. The first is made by cartesian meshes, labeled Cartesian and shown in Fig. 5(a). The second sequence, depicted in Fig. 5(b) and labeled

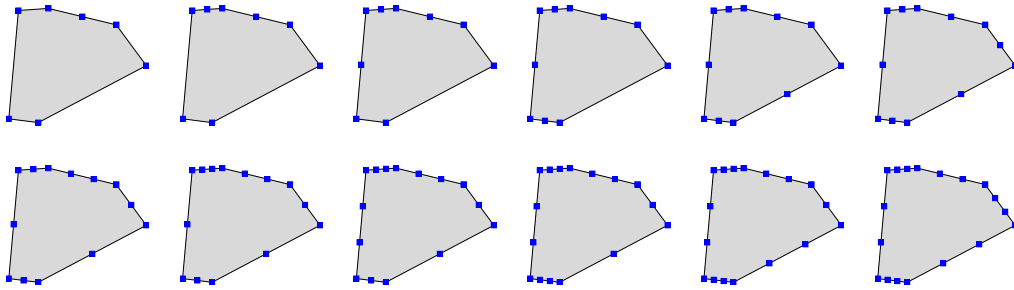


Fig. 3. Hexagons with aligned edges with  $N_E$  ranging from 7 to 18.

Table 13

Hexagon with aligned edges,  $k = 2$ . Values of  $\ell_E$  given by Algorithm 1, in parentheses the smallest value satisfying the necessary condition (76), and computed value of  $\sigma_E$ .

$N_E$	7	8	9	10	11	12	13	14
$\ell_E$	2 (2)	3 (3)	3 (3)	3 (3)	4 (4)	4 (4)	4 (4)	5 (4)
$\sigma_E$	5.8e-03	1.1e-02	9.5e-03	3.4e-03	2.8e-02	1.5e-02	2.1e-04	1.7e-04
$N_E$	15	16	17	18				
$\ell_E$	5 (5)	5 (5)	6 (5)	6 (5)				
$\sigma_E$	1.7e-04	1.1e-04	6.5e-04	5.2e-04				

Table 14

Hexagon with aligned edges,  $k = 3$ . Values of  $\ell_E$  given by Algorithm 1, in parentheses the smallest value satisfying the necessary condition (76), and computed value of  $\sigma_E$ .

$N_E$	7	8	9	10	11	12	13	14
$\ell_E$	3 (2)	3 (3)	3 (3)	4 (4)	4 (4)	5 (4)	5 (5)	6 (5)
$\sigma_E$	6.5e-03	5.6e-05	2.0e-07	1.4e-04	3.2e-06	5.8e-04	1.6e-06	1.4e-07
$N_E$	15	16	17	18				
$\ell_E$	6 (5)	7 (6)	7 (6)	8 (6)				
$\sigma_E$	6.3e-08	4.7e-07	1.3e-07	2.1e-06				

Table 15

Hexagon with aligned edges,  $k = 3$ . Increased values of  $\ell_E$  with respect to Table 14, in parentheses the smallest value satisfying the necessary condition (76), and computed value of  $\sigma_E$ .

$N_E$	9	9	$N_E$	14	14	$N_E$	16	16
$\ell_E$	3 (3)	4 (3)	$\ell_E$	6 (5)	7 (5)	$\ell_E$	7 (6)	8 (6)
$\sigma_E$	2.0e-07	2.3e-04	$\sigma_E$	1.4e-07	1.1e-06	$\sigma_E$	4.7e-07	3.8e-06
$N_E$	15	15	15		$N_E$	17	17	
$\ell_E$	6 (5)	7 (5)	8 (5)		$\ell_E$	7 (6)	8 (6)	
$\sigma_E$	6.3e-08	7.4e-07	5.6e-06		$\sigma_E$	1.3e-07	3.7e-06	

Table 16

Hexagon with aligned edges,  $k = 4$ . Values of  $\ell_E$  given by Algorithm 1, in parentheses the smallest value satisfying the necessary condition (76), and computed value of  $\sigma_E$ .

$N_E$	7	8	9	10	11	12	13	14
$\ell_E$	3 (2)	4 (3)	4 (3)	4 (4)	5 (4)	5 (5)	7 (5)	8 (6)
$\sigma_E$	3.0e-04	1.4e-06	5.2e-07	3.0e-07	1.0e-06	3.6e-07	1.5e-06	3.2e-07
$N_E$	15	16	17	18				
$\ell_E$	8 (6)	9 (6)	9 (7)	9 (7)				
$\sigma_E$	3.2e-07	1.7e-07	1.4e-07	2.0e-07				

**Table 17**

Hexagon with aligned edges,  $k = 4$ . Increased values of  $\ell_E$  with respect to Table 16, in parentheses the smallest value satisfying the necessary condition (76), and computed value of  $\sigma_E$ .

$N_E$	7	8	9	10	11	12	13	14
$\ell_E$	3 (2)	4 (3)	5 (3)	5 (4)	5 (4)	6 (5)	7 (5)	13 (6)
$\sigma_E$	3.0e-04	1.4e-06	6.7e-06	4.8e-06	1.0e-06	1.4e-05	1.5e-06	2.4e-06
$N_E$	15	16	17	18				
$\ell_E$	12 (6)	13 (6)	12 (7)	13 (7)				
$\sigma_E$	1.4-06	1.6e-06	1.2e-06	1.2e-06				

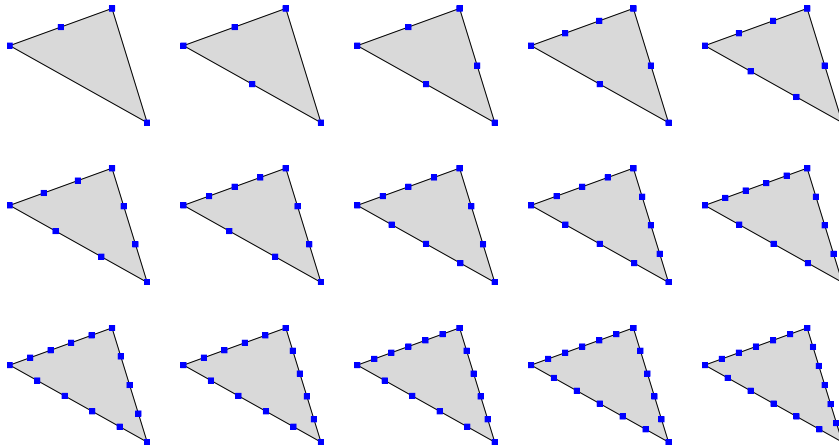


**Fig. 4.** Triangles with aligned edges with  $N_E$  ranging from 4 to 18.

**Table 18**

Triangles with aligned edges,  $k = 2$ . Values of  $\ell_E$  given by Algorithm 1, in parentheses the smallest value satisfying the necessary condition (76), and computed value of  $\sigma_E$ .

$N_E$	4	5	6	7	8	9	10	11
$\ell_E$	1 (1)	2 (1)	3 (2)	3 (2)	4 (3)	5 (3)	5 (3)	6 (4)
$\sigma_E$	3.7e-01	4.1e-01	3.9e-01	2.1e-01	2.4e-01	3.3e-01	1.0e-01	1.1e-01
$N_E$	12	13	14	15	16	17	18	
$\ell_E$	7 (4)	7 (4)	8 (4)	9 (5)	9 (5)	10 (5)	11 (5)	
$\sigma_E$	2.9e-01	4.3e-02	4.6e-02	2.0e-01	1.7e-02	1.7e-02	1.0e-01	

**Table 19**

Triangles with aligned edges,  $k = 3$ . Values of  $\ell_E$  given by Algorithm 1, in parentheses the smallest value satisfying the necessary condition (76), and computed value of  $\sigma_E$ .

$N_E$	4	5	6	7	8	9	10	11
$\ell_E$	2 (1)	3 (1)	4 (2)	5 (2)	6 (3)	6 (3)	8 (4)	9 (4)
$\sigma_E$	2.5e-01	2.8e-01	3.2e-01	9.5e-02	1.0e-01	7.1e-02	2.6e-02	2.6e-02
$N_E$	12	13	14	15	16	17	18	
$\ell_E$	10 (4)	11 (5)	12 (5)	12 (5)	14 (6)	15 (6)	16 (6)	
$\sigma_E$	1.2e-01	6.1e-03	6.0e-03	4.5e-03	2.6e-03	1.8e-03	1.2e-02	

**Table 20**

Triangles with aligned edges,  $k = 4$ . Values of  $\ell_E$  given by Algorithm 1, in parentheses the smallest value satisfying the necessary condition (76), and computed value of  $\sigma_E$ .

$N_E$	4	5	6	7	8	9	10	11
$\ell_E$	3 (1)	4 (1)	5 (2)	7 (2)	8 (3)	9 (3)	11 (4)	12 (4)
$\sigma_E$	1.6e-01	1.7e-01	2.8e-01	4.0e-02	4.0e-02	1.5e-01	5.8e-03	4.6e-03
$N_E$	12	13	14	15	16	17	18	
$\ell_E$	13 (5)	15 (5)	16 (6)	17 (6)	21 (6)	21 (7)	21 (7)	
$\sigma_E$	3.9e-02	3.3e-03	7.1e-03	1.6e-02	1.7e-01	1.8e-01	1.3e-01	

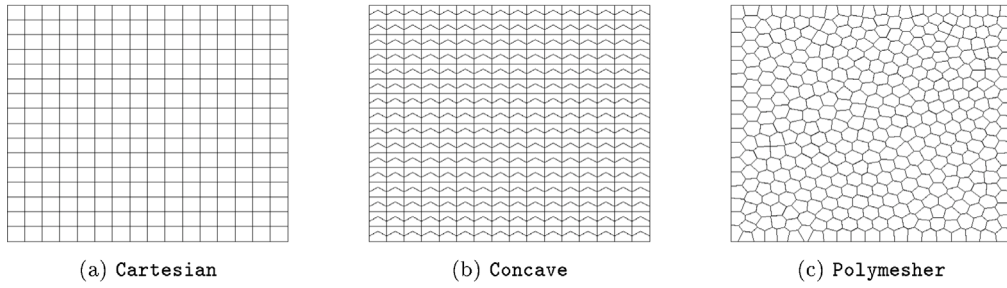


Fig. 5. Meshes used for convergence tests.

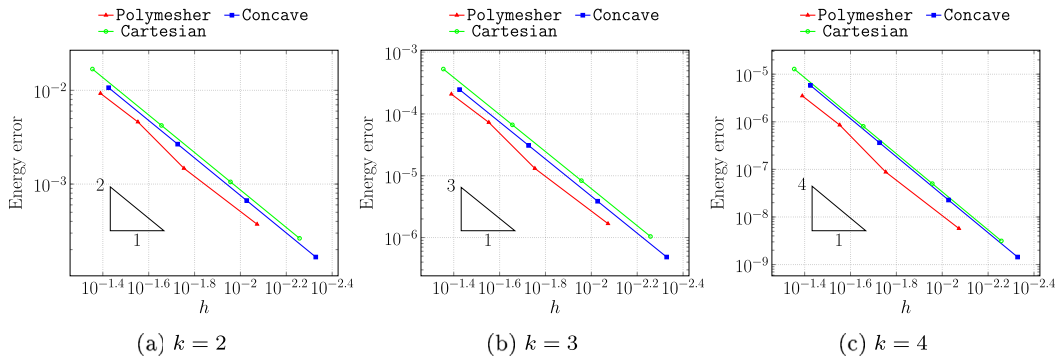


Fig. 6. Test 1: Convergence plots.

Concave, is made by pentagons, half of which are concave. Finally, the last family, shown in Fig. 5(c) and labeled Polymesher, is made by convex polygons, obtained using Polymesher [33].

For each test, we compute the discrete solution  $u_h$  for various orders of the method, in particular  $k = 2, 3, 4$ , and show the convergence curves of Energy and  $L^2$  errors, that we measure as follows

$$\text{Energy error}^2 = \frac{\sum_{E \in \mathcal{M}_h} \left\| \sqrt{\mathcal{K}} \left( \nabla \Pi_k^{\nabla, E} u_h - \nabla u \right) \right\|_{L^2(E)}^2 + \left\| \sqrt{\gamma} \left( \Pi_k^{\nabla, E} u_h - u \right) \right\|_{L^2(E)}^2}{\left\| \sqrt{\mathcal{K}} \nabla u \right\|_{L^2(\Omega)}^2 + \left\| \sqrt{\gamma} u \right\|_{L^2(\Omega)}^2},$$

$$\text{L}^2 \text{ error}^2 = \frac{\sum_{E \in \mathcal{M}_h} \left\| \Pi_k^{\nabla, E} u_h - u \right\|_{L^2(E)}^2}{\|u\|_{L^2(\Omega)}^2}.$$

The discrete solution  $u_h$  is obtained selecting locally on each polygon  $E$  the value  $\ell_E$  as described in Section 6, using the value of  $\ell_E$  provided by Algorithm 1.

7.2.1. Test 1

Let us consider problem (1) with

$$\mathcal{K} = \begin{pmatrix} 1 & 0 \\ 0 & 1 \end{pmatrix}, \quad \beta = \begin{pmatrix} 1 \\ 1 \end{pmatrix}, \quad \gamma = 1,$$

and the forcing term being such that the exact solution is  $u_{ex}(x, y) = \sin(2\pi x) \sin(2\pi y) + x$ . We consider Dirichlet conditions on  $\partial\Omega$  according to the exact solution. In Fig. 6, we report the trend of the Energy and  $L^2$  errors for all the families of meshes considered. The results are a numerical confirmation of the convergence rates proved in Section 5.

7.2.2. Test 2

Now, we want to analyze problem (1) where  $\mathcal{K} = \begin{pmatrix} 8 \cdot 10^{-3} & 0 \\ 0 & 1 \end{pmatrix}$  is an anisotropic diffusivity tensor,  $\beta = (0 \ 0)^T$  and  $\gamma = 0$ . We set Dirichlet boundary conditions and the forcing term such that the exact solution results  $u_{ex}(x, y) = 10^{-2}xy(1-x)(1-y)(e^{20x} - 1)$ . We compare the results given by the proposed method with the ones performed using a standard VEM method [2], where the discrete

problem is given by substituting in (25) the definition of the local bilinear form  $a_h^E$  with

$$a_h^E(u_h, v_h) = \left( \mathcal{K} \Pi_{k-1}^{0,E} \nabla u_h, \Pi_{k-1}^{0,E} \nabla v_h \right)_E + \|\mathcal{K}\|_{L^\infty(E)} S^E \left( (I - \Pi_k^{\nabla,E}) u_h, (I - \Pi_k^{\nabla,E}) v_h \right) \quad (77)$$

and  $S^E : \mathcal{V}_{h,k}^E \times \mathcal{V}_{h,k}^E \rightarrow \mathbb{R}$  denotes the local *dofi-dofi* stabilizing bilinear form

$$S^E(u_h, v_h) = \chi^E(u_h) \cdot \chi^E(v_h) \quad \forall u_h, v_h \in \mathcal{V}_{h,k}^E,$$

with  $\chi^E(v_h)$  defined as the vector of degrees of freedom of  $v_h$  on  $E$ . This stabilization is chosen since it is the most widely used in the VEM literature. In Fig. 7, we report the results obtained by the two methods in the case  $k = 2$ . In the captions, we refer to the proposed method with the acronym SFVEM and to the standard method with VEM. We observe that standard VEM displays larger errors in the case of Polymesher mesh, whereas the two methods behave equivalently in the case of Concave and Cartesian meshes. As also discussed in [18], these results can be related to the isotropic nature of the stabilization term, that can induces larger error when the mesh is not aligned with the principal directions of the anisotropy.

### 7.2.3. Test 3

With the same purpose of the previous test case, we now take into consideration a case where  $\mathcal{K} = \begin{pmatrix} 1 & 0 \\ 0 & 6.25 \cdot 10^{-4} \end{pmatrix}$ ,  $\beta = (0 \ 0)^T$  and  $\gamma = 0$ . We impose Dirichlet boundary conditions and the forcing term such that the exact solution results  $u_{ex}(x, y) = \sin(2\pi x) \sin(80\pi y)$ . We depict the convergence results for the two analyzed methods with  $k = 2$  in Fig. 8. We observe that as in the previous test, differences between the two methods' behavior appear when the mesh is not aligned with the anisotropy, i.e. when Polymesher meshes are used. Moreover, due to the very strong anisotropy of the solution, we see in 8(a) and 8(b) that the proposed method reaches the expected asymptotic regime before the standard VEM.

## Conclusions

In this work, we propose a high-order virtual element scheme for a 2D second order elliptic equation, that do not require an arbitrary stabilizing term. It is based on the definition of high-order polynomial projections that induce the existence of consistent and stable bilinear forms. The well-posedness is proved and optimal a priori error estimates are derived, identifying a necessary and sufficient condition on the projection polynomial space. We propose an algorithm to provide the polynomial projection degree ensuring stability, based on a local incremental QR decomposition. Numerical tests on polygons with several different shapes confirm the local stability of the method and validate the proposed algorithm. Finally, we perform convergence test to assess the robustness of the proposed method, especially in problems characterized by anisotropic diffusion and solutions. We compare the performance with a stabilized VEM scheme and results on meshes that are not aligned with anisotropies show that a structure-preserving scheme can reduce the magnitude of the error and help convergence.

## CRedit authorship contribution statement

**Stefano Berrone:** Writing – review & editing, Writing – original draft, Validation, Supervision, Software, Resources, Methodology, Investigation, Funding acquisition, Formal analysis, Conceptualization. **Andrea Borio:** Writing – review & editing, Writing – original draft, Validation, Supervision, Software, Resources, Methodology, Formal analysis, Conceptualization. **Davide Fassino:** Writing – review & editing, Writing – original draft, Validation, Software, Methodology, Investigation, Formal analysis, Conceptualization. **Francesca Marcon:** Writing – review & editing, Writing – original draft, Validation, Software, Methodology, Investigation, Formal analysis, Conceptualization.

## Declaration of competing interest

The authors declare that they have no known competing financial interests or personal relationships that could have appeared to influence the work reported in this paper.

## Acknowledgments

The four authors are members of the Gruppo Nazionale Calcolo Scientifico (GNCS) at Istituto Nazionale di Alta Matematica (INdAM). The authors kindly acknowledge financial support by INdAM-GNCS Project 2024 (CUP: E53C23001670001), by the Italian Ministry of University and Research (MUR) through the project MUR-M4C2-1.1- PRIN 2022 (CUP: E53D23005820006), and by the European Union through Next Generation EU, M4C2, PRIN 2022 PNRR project (CUP: E53D23017950001) and PNRR M4C2 project of CN00000013 National Centre for HPC, Big Data and Quantum Computing (HPC) (CUP: E13C22000990001).

## Data availability

Data will be made available on request.

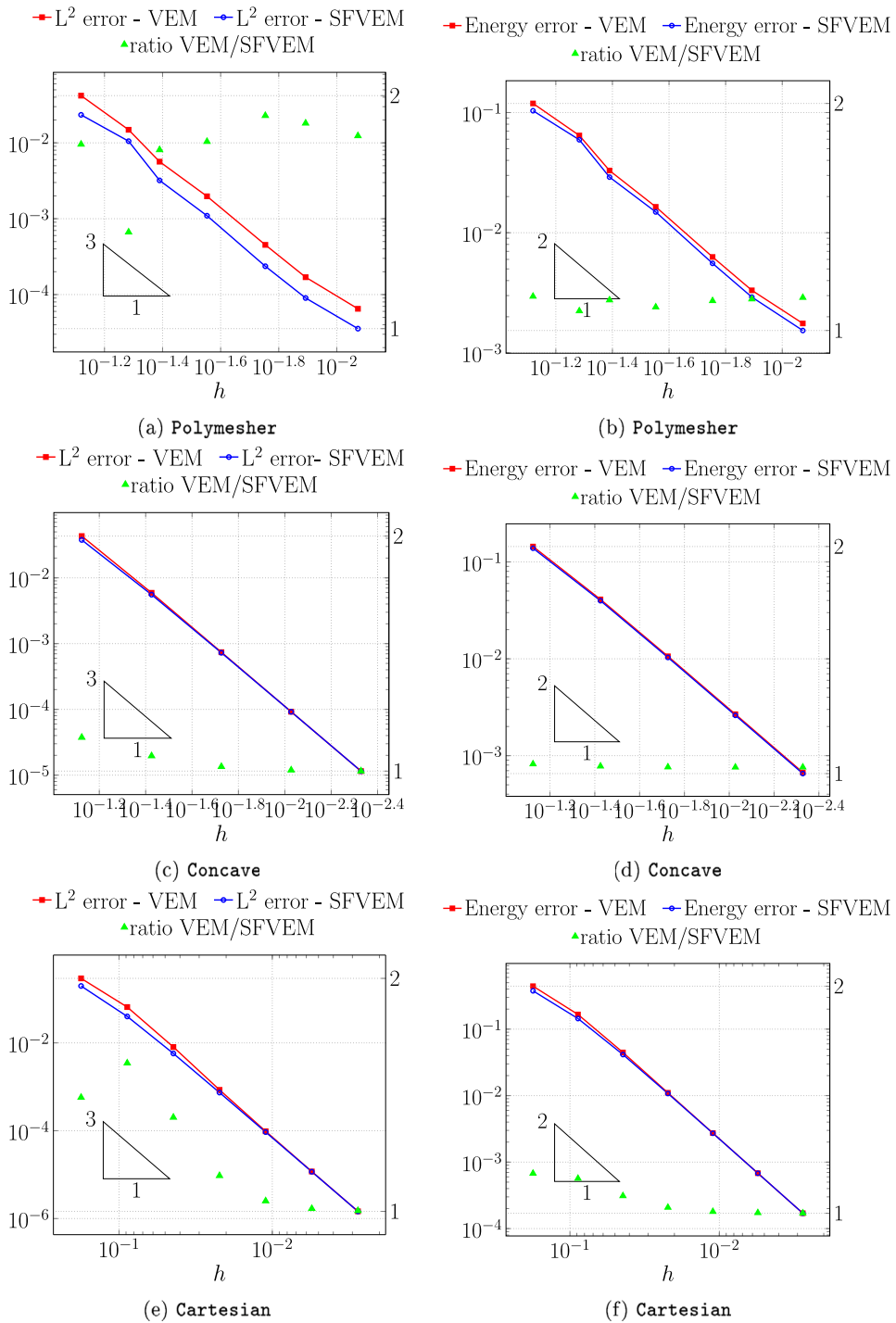


Fig. 7. Test 2: Convergence plots. In each figure, the  $y$ -axis on the left refers to the errors, while the  $y$ -axis on the right refers to the ratio between the errors made by the two methods.

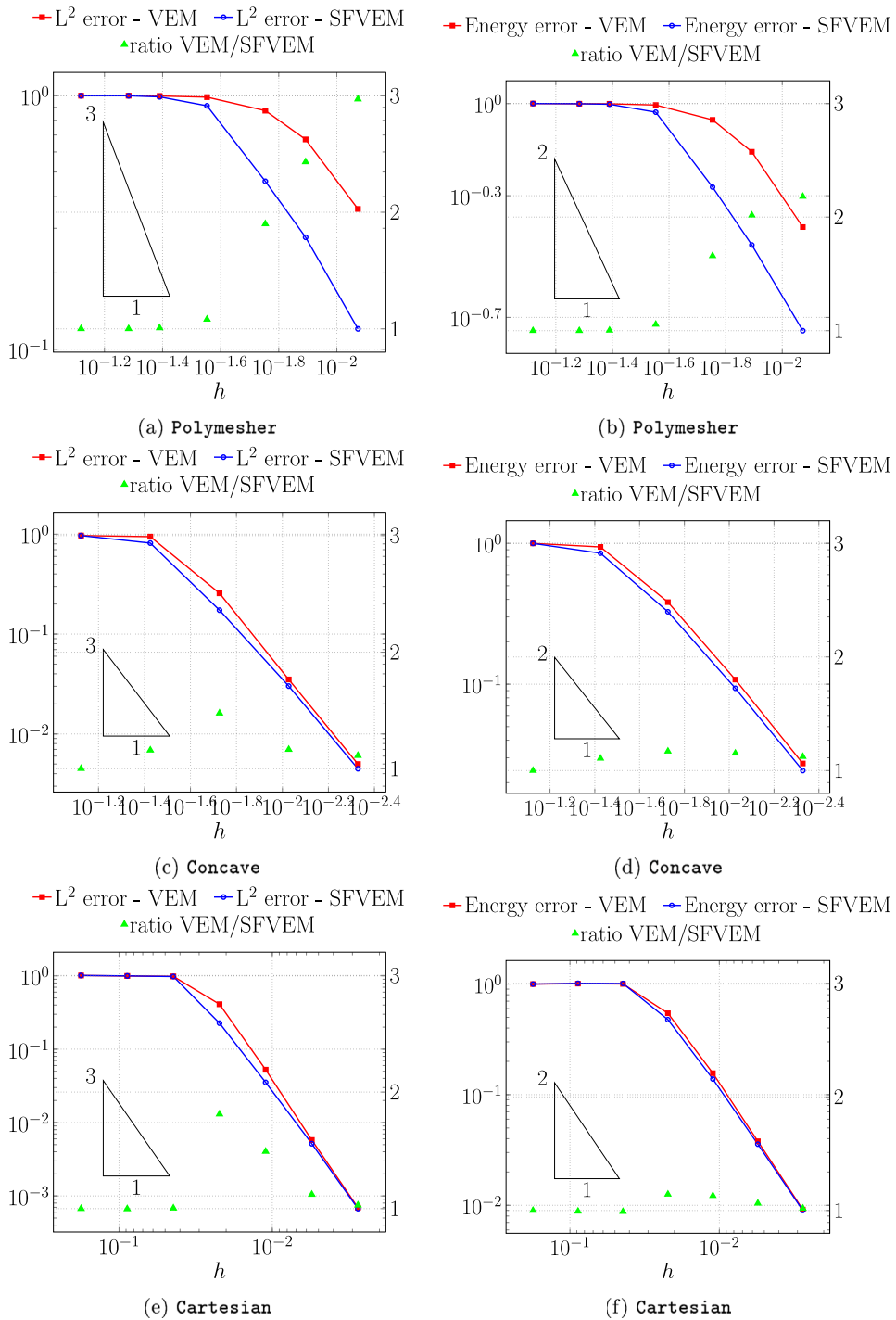


Fig. 8. Test 3: Convergence plots. In each figure, the y-axis on the left refers to the errors, while the y-axis on the right refers to the ratio between the errors made by the two methods.

References

[1] L. Beirão da Veiga, F. Brezzi, A. Cangiani, G. Manzini, L.D. Marini, A. Russo, Basic principles of virtual element methods, Math. Models Methods Appl. Sci. 23 (01) (2013) 199–214, <http://dx.doi.org/10.1142/S0218202512500492>.

- [2] L. Beirão da Veiga, F. Brezzi, L.D. Marini, A. Russo, Virtual element methods for general second order elliptic problems on polygonal meshes, *Math. Models Methods Appl. Sci.* 26 (04) (2015) 729–750, <http://dx.doi.org/10.1142/S0218202516500160>.
- [3] M.F. Benedetto, S. Berrone, A. Borio, S. Pieraccini, S. Scialò, Order preserving SUPG stabilization for the virtual element formulation of advection-diffusion problems, *Comput. Methods Appl. Mech. Engrg.* 311 (2016) 18–40, <http://dx.doi.org/10.1016/j.cma.2016.07.043>.
- [4] S. Berrone, A. Borio, G. Manzini, SUPG stabilization for the nonconforming virtual element method for advection–diffusion–reaction equations, *Comput. Methods Appl. Mech. Engrg.* 340 (2018) 500–529, <http://dx.doi.org/10.1016/j.cma.2018.05.027>.
- [5] A. Cangiani, G. Manzini, O.J. Sutton, Conforming and nonconforming virtual element methods for elliptic problems, *IMA J. Numer. Anal.* 37 (3) (2016) 1317–1354, <http://dx.doi.org/10.1093/imanum/drw036>.
- [6] S. Berrone, A. Borio, A residual a posteriori error estimate for the virtual element method, *Math. Models Methods Appl. Sci.* 27 (08) (2017) 1423–1458, <http://dx.doi.org/10.1142/S0218202517500233>.
- [7] F. Credali, S. Bertoluzza, D. Prada, Reduced basis stabilization and post-processing for the virtual element method, *Comput. Methods Appl. Mech. Engrg.* 420 (2024) 116693, <http://dx.doi.org/10.1016/j.cma.2023.116693>.
- [8] L. Beirão da Veiga, C. Canuto, R.H. Nochetto, G. Vacca, M. Verani, Adaptive vem: Stabilization-free a posteriori error analysis and contraction property, *SIAM J. Numer. Anal.* 61 (2) (2023) 457–494, <http://dx.doi.org/10.1137/21M1458740>.
- [9] C. Canuto, D. Fassino, Higher-order adaptive virtual element methods with contraction properties, *Math. Eng.* 5 (6) (2023) 1–33, <http://dx.doi.org/10.3934/mine.2023101>.
- [10] S. Berrone, D. Fassino, F. Vicini, 3D adaptive VEM with stabilization-free a posteriori error bounds, 2024, [arXiv:2407.17858](https://arxiv.org/abs/2407.17858).
- [11] A. Russo, N. Sukumar, Quantitative study of the stabilization parameter in the virtual element method, in: H. Beirão da Veiga, F. Minhós, N. Van Goethem, L. Sanchez Rodrigues (Eds.), *Nonlinear Differential Equations and Applications*, Springer International Publishing, Cham, 2024, pp. 259–278, [http://dx.doi.org/10.1007/978-3-031-53740-0\\_14](http://dx.doi.org/10.1007/978-3-031-53740-0_14).
- [12] D. Boffi, F. Gardini, L. Gastaldi, Approximation of PDE eigenvalue problems involving parameter dependent matrices, *Calcolo* 57 (4) (2020) <http://dx.doi.org/10.1007/s10092-020-00390-6>.
- [13] A. D’Altri, S. de Miranda, L. Patruno, E. Sacco, An enhanced VEM formulation for plane elasticity, *Comput. Methods Appl. Mech. Engrg.* 376 (2021) 113663, <http://dx.doi.org/10.1016/j.cma.2020.113663>.
- [14] S. Berrone, A. Borio, F. Marcon, G. Teora, A first-order stabilization-free virtual element method, *Appl. Math. Lett.* 142 (2023) 108641, <http://dx.doi.org/10.1016/j.aml.2023.108641>.
- [15] A. Lamperti, M. Cremonesi, U. Perego, C. Lovadina, A. Russo, A Hu-Washizu variational approach to self-stabilized Virtual Elements: 2D linear elastostatics, *Comput. Mech.* 71 (2023) 935–955, <http://dx.doi.org/10.1007/s00466-023-02282-2>.
- [16] A. Borio, C. Lovadina, F. Marcon, M. Visinoni, A lowest order stabilization-free mixed virtual element method, *Comput. Math. Appl.* 160 (2024) 161–170, <http://dx.doi.org/10.1016/j.camwa.2024.02.024>.
- [17] S. Berrone, A. Borio, F. Marcon, A stabilization-free virtual element method based on divergence-free projections, *Comput. Methods Appl. Mech. Engrg.* 424 (2024) 116885, <http://dx.doi.org/10.1016/j.cma.2024.116885>.
- [18] S. Berrone, A. Borio, F. Marcon, Comparison of standard and stabilization free virtual elements on anisotropic elliptic problems, *Appl. Math. Lett.* 129 (2022) 107971, <http://dx.doi.org/10.1016/j.aml.2022.107971>.
- [19] A. Chen, N. Sukumar, Stabilization-free virtual element method for plane elasticity, *Comput. Math. Appl.* 138 (2023) 88–105, <http://dx.doi.org/10.1016/j.camwa.2023.03.002>.
- [20] A. Chen, N. Sukumar, Stabilization-free serendipity virtual element method for plane elasticity, *Comput. Methods Appl. Mech. Engrg.* 404 (2023) 115784, <http://dx.doi.org/10.1016/j.cma.2022.115784>.
- [21] B. Xu, P. Wriggers, 3D stabilization-free virtual element method for linear elastic analysis, *Comput. Methods Appl. Mech. Engrg.* 421 (2024) 116826, <http://dx.doi.org/10.1016/j.cma.2024.116826>.
- [22] A. Borio, M. Busetto, F. Marcon, Supg-stabilized stabilization-free vem: a numerical investigation, *Math. Eng.* 6 (1) (2024) 173–191, <http://dx.doi.org/10.3934/mine.2024008>.
- [23] B. Xu, Y. Wang, P. Wriggers, Stabilization-free virtual element method for finite strain applications, *Comput. Methods Appl. Mech. Engrg.* 417 (2023) 116555, <http://dx.doi.org/10.1016/j.cma.2023.116555>.
- [24] B. Xu, Y. Wang, P. Wriggers, Stabilization-free virtual element method for 2D elastoplastic problems, *Internat. J. Numer. Methods Engrg.* (2024) e7490, <http://dx.doi.org/10.1002/nme.7490>.
- [25] F. Liguori, A. Madeo, S. Marfia, G. Garcea, E. Sacco, A stabilization-free hybrid virtual element formulation for the accurate analysis of 2D elasto-plastic problems, *Comput. Methods Appl. Mech. Engrg.* 431 (2024) 117281, <http://dx.doi.org/10.1016/j.cma.2024.117281>.
- [26] B. Ahmad, A. Alsaedi, F. Brezzi, L.D. Marini, A. Russo, Equivalent projectors for virtual element methods, *Comput. Math. Appl.* 66 (2013) 376–391, <http://dx.doi.org/10.1016/j.camwa.2013.05.015>.
- [27] D. Boffi, F. Brezzi, M. Fortin, *Mixed Finite Element Methods and Applications*, in: Springer Series in Computational Mathematics, Springer, 2013, <http://dx.doi.org/10.1007/978-3-642-36519-5>.
- [28] L. Beirão da Veiga, C. Lovadina, A. Russo, Stability analysis for the virtual element method, *Math. Models Methods Appl. Sci.* 27 (13) (2017) 2557–2594, <http://dx.doi.org/10.1142/S021820251750052X>.
- [29] S.C. Brenner, L.-Y. Sung, Virtual element methods on meshes with small edges or faces, *Math. Models Methods Appl. Sci.* 28 (07) (2018) 1291–1336, <http://dx.doi.org/10.1142/S0218202518500355>.
- [30] Veiga, Dassi, . and Franco, Lovadina, . and Carlo, Vacca, . and Giuseppe, Supg-stabilized virtual elements for diffusion-convection problems: a robustness analysis, *ESAIM: M2AN* 55 (5) (2021) 2233–2258, <http://dx.doi.org/10.1051/m2an/2021050>.
- [31] A. Cangiani, E.H. Georgoulis, T. Pryer, O.J. Sutton, A posteriori error estimates for the virtual element method, *Numer. Math.* 137 (4) (2017) 857–893, <http://dx.doi.org/10.1007/s00211-017-0891-9>.
- [32] M. Cicuttin, An implementation detail about the scaling of monomial bases in polytopal finite element methods, *Appl. Math. Lett.* 159 (2025) 109281, <http://dx.doi.org/10.1016/j.aml.2024.109281>.
- [33] C. Talischi, G.H. Paulino, A. Pereira, I.F.M. Menezes, Polymesh: A general-purpose mesh generator for polygonal elements written in matlab, *Struct. Multidiscipl. Optim.* 45 (3) (2012) 309–328, <http://dx.doi.org/10.1007/s00158-011-0706-z>.